Study of the VFE discretisation in view of NH modeling

P. BÉNARD

Centre National de Recherches Météorologiques, Météo-France, Toulouse, France

Version 1

7 December 2004

(file : vfememo1.tex)

This paper is a working document, which can serve as a starting basis for discussions between ECMWF and Météo-France about the extension of the current IFS Vertical Finite Elements (VFE) scheme to NH modelling. This paper is the first version of a paper which by definition should be subject to significant modifications through discussions.

ABSTRACT

The current VFE discretisation introduced in IFS by ECMWF for the HPE system is examined, in view of its extension the NH system trying to avoid major changes in the existing dynamical kernel of the model.
The aspects covered by this paper are :

- Detailed scientific description of IFS's VFE discretisation
- Some limitations and a weakness in the current VFE discretisation
- Possible avenues for the extension of the VFE scheme to NH modelling
- Behaviour of the current VFE scheme and of the proposed avenues (accuracy, normal modes, ...)

It is found that very few possibilities are able to simultaneously satisfy feasability, accuracy and stability. In this preliminary study, only the most scientifically simple and technically straightforward extensions of the HPE-VFE scheme to the NH-VFE scheme have been examined. Some alternative options which are scientifically more ambitious have been left unexamined for time being, because the scope of this paper is more to evaluate if the extension of the HPE-VFE to NH-VFE is a straightforward technical issue or a longer term, scientifically uncertain one. Among all the straightforward possibilities examined , only one has been found able to be practically useable, and in spite of its technical feasbility and its stability, it does not offer the perspective of an high accuracy-order as would be allowed by a full use of the VFE technique in all spatial operators.
Alternative strategies are also reviewed. These alternative strategies require, at variable degrees, some scientific work to be undertaken. When possible, the degree of chance for their success is discussed.
The present study is restricted to the behaviour of the purely linear system associated to the SI scheme. The study of the behaviour of VFE schemes in presence of non-linear terms, more demanding in time, is left for a later stage, when a reasonable consensus on the way to proceed will have been reached.

---

1 Introduction

This paper examines the various possibilities for extending the HPE-VFE scheme of the current IFS model to a VFE scheme for NH modelling in a general framework close from the one of the current Aladin-NH dynamical kernel.
The VFE scheme of IFS has been described in Untch and Hortal, 2004 (UH04 hereafter). In the present memo, first, some relevant details of this discretisation (as implemented in IFS code) are discussed, namely, when the code implementation departs from the scheme described in UH04. Possible avenues for extending the VFE scheme to the NH version of the model are then explored and discussed. The most important properties of the current and proposed VFE schemes are presented, and compared to the equivalent properties obtained with the classical Finite-Differences (FD) scheme.

Notations :

Following the traditional notation always used in ARPEGE and IFS, the number of discrete nodes or levels is noted L throughout the present paper. This number was noted N in UH04, but this latter notation is not adopted here, for consistency with all previous documentations.
Consistently with existing NH documentations and papers, the hydrostatic pressure is noted π, the notation p being dedicated to the true pressure only. For an hydrostatic model, these two concepts are identical.

2 Description

Some details which are not completely clear from the UH04 paper (or different between the code and UH04) are described. The appropriate notations are introduced (to stick with both UH04 and Mathematica bed-test).

2.1 Differences with the UH04 paper

After examination of the IFS code (subroutine `SUVERTFE3.F90`) we found some differences with the UH04 paper which are worth being mentioned :

- The normalisation of functions e_i in IFS code is not the one described in UH04. The normalisation of IFS code is that the value of the element at the central node is 2/3. The effect is that for a regular spacing of levels and a unit function $f(\eta) = 1$, the total columun integral computed with VFE scheme should be one, i.e. $\left[\int_0^1 \mathbf{f}(\eta) d\eta\right]_{\text{VFE}} = 1$. This modification with respect to UH04 paper has no scientific impact.

- The shape of the e_i functions for $i \in \{L-1, L, L+1, L+2\}$ is modified for $\eta > \eta(L)$ in such a way that these functions become constant-valued below this limit. This modification is omitted in UH04, and probably only has a small impact on the behaviour of the scheme. As a direct consequence, the last node function e_{L+2} becomes identically zero. However, the relevance of having one of the basis function identically zero may be questionned. The shape of the functions modified as in the IFS code is depicted in Fig.1, for a 50 regularly spaced level distribution.

- The integral domain for the Galerkin test method is not set to $[0,1]$ as indicated in Eq. (3.7) of UH04, but is set to $[0, \eta_{(L+1)}]$. However, this domain for the mathematical transform must be clearly distinguished from the domain used for physical integrations as in Eq. (3.5) of UH04,

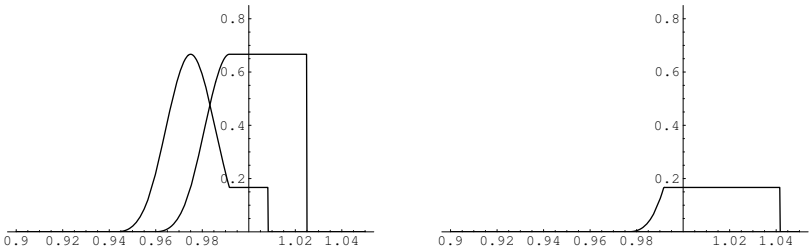

FIG. 1 – *Shape of the four bottom-most nodes functions, as modified in the IFS code or a 50 level uniform resolution. First panel : e_{L-1}, e_L. Second panel e_{L+1}. The last node function e_{L+2} is identically zero*

which is actually taken as $[0,1]$ when an integral through the whole vertical column is computed. This modification is not likely to change the results significantly, but it is not totally impact-free.

- For the node $i+2$, the function f_4 valid in the interval $[\eta_{i+1},\eta_{i+2}]$ is defined by $f_4(\eta) = a_4(\eta - \eta_{i+2})^3$. The formula in Eq. (A.3) UH04 has a typo, but the version in the code is correct (f_4 as defined in UH04 would result in a discontinuous basis-function).

- The index intervals for j in Eq. (3.10) in UH04 are wrong . The central equation must not be applied for $-1 \leq j \leq L+2$, but for $0 \leq j \leq L$. The last equation must not be applied to $L+2$ but to $L+1$. Therefore the last equation must read :

$$\sum_{i=-1}^{L+2} c_i e_i'(\eta_{L+1}) = f_{L+1}' \tag{1}$$

- In IFS code all the basic matrices **A**, **B**, **P**, **S** are dimensioned $[1,L+3]\times[1,L+3]$. The basic matrix $\mathbf{ZINTE} = \mathbf{P}.\mathbf{A}^{-1}.\mathbf{B}.\mathbf{S}^{-1}$ is called `ZINTE` in the code. However, this $[1,L+3]\times[1,L+3]$ matrix may not directly applied to a column vector, which by definition is dimensioned $[1,L]$. A projection is therefore applied (using some of the "physical" rules in the second paragraph of UH04's page 1512). A physical matrix that will be noted "**RINTE**" is thus built from **ZINTE** by :

  - removing the first and last lines of **ZINTE** (these lines would give the derivatives of the function at the two edges, which are not used).

  - removing the first and last column of **ZINTE** (these columns are to include the information about the vertical derivatives of the input vector at the two edges. Since these derivatives are readily assumed to be zero, these two columns are useless because they have no contribution for any input vector).

  - adding together the second and third columns of **ZINTE** and set the result as the first column of **RINTE** (the second column is the contribution of the input vector at the level η_0. Since the value of the vector there is readily assumed to be equal to the value at the level η_1, the two columns can be added together, and the initial second column of **ZINTE** can thus be ignored).

The physical matrix **RINTE** is therefore dimensioned $[1,L]\times[1,L+1]$ The last line, with index $L+1$ gives the total column integral from the whole vertical domain ($\eta=0$ to $\eta=1$ in the current code). The matrix **RINTE** is the basic output of the `SUVERTFE3` subroutine and is called `RINTE` in the code.

2.2 Correction of mass and hydrostatic-height elements

The discrete mass element $\delta\pi/\delta\eta$ reflecting UH04's Eq. (2.8) and its logarithm $\delta\ln\pi/\delta\eta$, are not defined from the specified A and B vectors through a direct FD differentiation, but they are defined through a VFE approach in such a way that the constraints (2.9) in UH04 are fulfilled at the computer accuracy. These quantities $\delta\pi/\delta\eta$ and $\delta\ln\pi/\delta\eta$ are needed for the integration of the mass-continuity equation (to compute the vertical pseudo-velocities) and of the hydrostatic equation (to compute the geopotential). However, this process is not described at all in UH04.
At the setup stage of the model, corrected profiles for quantities related to A and B are prepared. This involves corrected values for ($\delta A/\delta\eta$, $\delta B/\delta\eta$, A, B) at full levels. Then at each time-step, and for each column of the model, the local mass-elements ($\delta\pi/\delta\eta$, π, $\delta\ln\pi/\delta\eta$) are computed at full levels. The principle of this correction is now explained in details.

• At the setup stage of the model :

- Define $\delta A/\delta\eta$ and $\delta B/\delta\eta$ in the usual FD way,

- Integrate these quantities through the whole column,

- for correcting $(\delta B/\delta\eta)$, divide the original $(\delta B/\delta\eta)$ vector by the obtained column integral [we obtain a corrected vector $(\widehat{\delta B/\delta\eta})$] :

$$(\widehat{\delta B/\delta\eta}) = (\delta B/\delta\eta)\,/\!\!\int_0^1 (\delta B/\delta\eta)d\eta \tag{2}$$

(the notation of the integral operator in the above equation is adopted throughout all this paper for the VFE integral, in order to better distinguish from the continuous integral).

- for correcting $(\delta A/\delta\eta)$, use an iterative process to correct the original vector : detect the first level $l_{\rm ref}$ from top where $(\delta A/\delta\eta)$ changes its sign ; compute the vertical (positive) integral $I^+_{\rm ref}$ of $(\delta A/\delta\eta)$ between the top and $l_{\rm ref}$, and the (negative) integral form $I^-_{\rm ref}$ to the bottom ; multiply $(\delta A/\delta\eta)$ by $(-I^+_{\rm ref}/I^-_{\rm ref})$. Do this rapidly converging iterative process three times [we obtain a corrected vector $(\widehat{\delta A/\delta\eta})$].

- Define B at full levels by the VFE integral of the corrected $(\widehat{\delta B/\delta\eta})$ vector (we obtain a corrected vector $\widehat{B}$).

- Define A at full levels by the VFE integral of the corrected $(\widehat{\delta A/\delta\eta})$ vector (we obtain a corrected vector $\widehat{A}$).

• For each time-step and each column :

- Define the corrected full-level pressure depth $(\widehat{\delta\pi/\delta\eta})$ from $(\widehat{\delta A/\delta\eta})$, $(\widehat{\delta B/\delta\eta})$ and π_s.

- Define the pressure at full level $\widehat{\pi}$ from $\widehat{A}$, $\widehat{B}$ and π_s.

- Define the corrected logarithmic depth $(\widehat{\delta\ln\pi/\delta\eta})$ as $(\widehat{\delta\pi/\delta\eta})/\widehat{\pi}$.

This procedure garantees that, to the computer accuracy :

$$\widehat{\pi_l} = \int_0^{\eta_l} (\widehat{\delta\pi/\delta\eta}) d\eta \tag{3}$$

$$\pi_s = \int_0^{1} (\widehat{\delta\pi/\delta\eta}) d\eta \tag{4}$$

Note : A similar computation must also be performed for the SI reference surface pressure π_s^*. The corresponding vectors $\widehat{\pi^*}$, $\widehat{\delta\pi^*/\delta\eta}$ and $\widehat{\delta \ln \pi^*/\delta\eta}$ are needed in the SI linear system, to define the linear operators for the integration of the continuity and the hydrostatic equation, namely, the adimensional $\mathbf{G}^*$, $\mathbf{S}^*$ and $\mathbf{N}^*$ operators in the notation of the NH model (see also definition below). However, since π_s^* is not space- or time-dependent, the computation of these three vectors can be performed once, in the set-up stage of the model.

3 A weakness in the current VFE discretisation

For a given valid set of (A,B) values, the current VFE discretisation sometimes result in eigenmodes of the $\mathbf{\Gamma}$ matrix [i.e. the Γ operator in UH04's (4.7)] with complex or negative eigenvalues, which means that the normal modes of the model are unstable. The FD discretisation does not suffer from this weakness, and seems to provides positive eigenvalues in any case, when the set (A,B) defines a valid coordinate (i.e. monotonic with respect to z).

The instability is not linked to the hybrid character of the coordinate and appears even in the case of a pure terrain-following σ coordinate (i.e. $A \equiv 0$). Some investigations showed that the appearance of unstable modes is somehow linked to the existence of significant jumps in the pressure or height resolution from one level to the next.

More specifically, in the case of a NWP type discretisation (high-resolution in geopotential near the ground, and high-resolution in pressure near the top), the scheme was found highly sensitive to the ratio between the number of levels L_{250} in the "stratosphere" (i.e. above 250 hPa) and the pressure of the first full level. For instance, with $L_{250} = 18$, the scheme is easily made stable with $p_1 = 30$ Pa, while for $p_1 = 20$ Pa or less, it was found difficult (not to say impossible) to make it stable. This behaviour is found to be quite independent of the positioning of the levels underneath. Similarly, in order to reach a first full-level pressure of $p_1 = 10$ Pa, a minimum of 26 levels above 250 Pa seems more or less necessary.

As an other illustration, the simple 8-levels terrain-following σ coordinate defined by $A = 0$ and $B = \{0, 0.007, 0.03, 0.07, 0.15, 0.30, 0.50, 0.75, 1\}$, leads to an operator $\mathbf{\Gamma}$ which has complex eigenvalues, and therefore to an unstable model. Moreover, the imaginary part of these complex eigenvalues is not negligible. Here also, in contratst, the FD discretisation provides only real positive eigenvalues for $\mathbf{\Gamma}$.

It would be interesting to investigate more deeply why the VFE discretisation sometimes behaves unstably while the FD discretisation does not exhibit this pathological behaviour. The modifications brought near the two edges throughout the whole depth of the domain may be in cause. A more fundamental cause could be in the very indirect way in which the integration operator is obtained, with matrix inversions involved in the process.

4 Some limitations in the current VFE discretisation

The current VFE discretisation, as it appears in the code, is mostly operation-oriented. However, for the theoretical understanding of the behaviour of the scheme, and for academic studies, more general

extensions could be needed.

4.1 Extension to pure terrain-following coordinates

The current VFE discretisation is not able to support pure terrain-following coordinates (i.e. $A \equiv 0$). In this case, the correction of the $(dA/d\eta)$ function implies a division by 0 in the current code, and this problem should be avoided by simply skipping this correction when $A \equiv 0$. This represents a very small code modification.

4.2 Extension to bounded domains

The current VFE discretisation is restricted to unbounded domains, i.e. the domain top pressure π_T is assumed to be zero. Due to UH04's (2.6), this means that $A_T = B_T = 0$, and UH04's (3.1) implies $\eta_T = 0$. However, for academic modelling, intercomparison studies, and for theoretical studies, it may be important to allow vertically bounded domains for which π_T and η_T are allowed to be non-zero. This can be achieved by allowing A_T and/or B_T to be non-zero. The particular case of a bounded domain in terrain-following coordinate is obtained by $A \equiv 0$ and $B_T \neq 0$.

In all this paper (except in the space-continuous derivations), we assume that η_T is allowed to be non-zero, and therefore we introduce the proper formalism for it. The surface value of η is kept as one [as imposed by UH04's (2.6)].

5 Main vertical operators involved in the model

5.1 Basic integral operators

The basic integral operators, defined as output of the VFE scheme, are the total column integral $\mathscr{K}$ and the integral though the top to the current level $\mathscr{J}$:

$$(\mathscr{K}X)_\eta = \int_{\eta_T}^{1} X(\eta')d\eta' \tag{5}$$

$$(\mathscr{J}X)_\eta = \int_{\eta_T}^{\eta} X(\eta')d\eta' \tag{6}$$

We also define, for convenience, the identity operator :

$$(\mathscr{I}X)_\eta = X(\eta) \tag{7}$$

Note that $\mathscr{K}X$, as defined here, returns a function (not a value) in the whole vertical domain (this function is however vertically uniform).
The discrete VFE counterparts of these operators are noted **K**, **J** and **I** respectively :

$$(\mathbf{K}X)_{\eta_l} = \int_{\eta_T}^{1} X(\eta'_l)d\eta' \tag{8}$$

$$(\mathbf{J}X)_{\eta_l} = \int_{\eta_T}^{\eta_l} X(\eta'_l)d\eta' \tag{9}$$

$$(\mathbf{I}X)_{\eta_l} = X(\eta_l) \tag{10}$$

Therefore, **K** is obtained by vertically stacking L times the row vector formed by the last line of **RINTE**, and **J** is obtained by taking the first L lines of **RINTE**. The operator **J** thus provides for any given vector $[1,L]$, the integral of the vector on each of the $[1,L]$ full levels, and the operator **K** provides for any given vector $[1,L]$, the total column integral of the vector, and puts the result identically on each of the $[1,L]$ full levels.

For convenience, let's define other various discrete square $[1,L]\times[1,L]$ operators needed for later derivations :

- $\mathbf{\Pi}$: square diagonal operator with the non-zero element $\widehat{\pi}$ at each full level (and $\mathbf{\Pi}^{-1}$ its inverse).
- $\mathbf{d\Pi}$: square diagonal operator with the element $(\widehat{\delta\pi/\delta\eta})$ at each full level.
- $\mathbf{dL\Pi}$: square diagonal operator with the element $(\widehat{\delta\ln\pi/\delta\eta})$ at each full level (therefore $\mathbf{dL\Pi} = \mathbf{d\Pi}.\mathbf{\Pi}^{-1}$).

5.2 Mass-weighted operators

For a given η coordinate, the continuous basic linear mass-weighted operators write :

$$(\mathscr{G}^*X)_\eta = \int_\eta^1 \frac{d\ln\pi^*}{d\eta'}X(\eta')d\eta' \tag{11}$$

$$(\mathscr{S}^*X)_\eta = \frac{1}{\pi^*}\int_{\eta_T}^\eta \frac{d\pi^*}{d\eta'}X(\eta')d\eta' \tag{12}$$

$$(\mathscr{N}^*X)_\eta = \frac{1}{\pi_s^*}\int_{\eta_T}^1 \frac{d\pi^*}{d\eta'}X(\eta')d\eta' \tag{13}$$

These continuous operators represent the operators needed in Eqs. (4.4)–(4.6) of UH04 (note that for continuous operators, the corrected height- and mass-elements do not need to be introduced).
The non-linear counterpart of these continuous operators are :

$$(\mathscr{G}X)_\eta = \int_\eta^1 \frac{d\ln\pi}{d\eta'}X(\eta')d\eta' \tag{14}$$

$$(\mathscr{S}X)_\eta = \frac{1}{\pi}\int_{\eta_T}^\eta \frac{d\pi}{d\eta'}X(\eta')d\eta' \tag{15}$$

$$(\mathscr{N}X)_\eta = \frac{1}{\pi_s}\int_{\eta_T}^1 \frac{d\pi}{d\eta'}X(\eta')d\eta' \tag{16}$$

These continuous operators represent the operators needed in Eqs. (2.5) and (2.10)–(2.13) of UH04.

The discrete version of these operators is derived in a natural way from the basic integral operators **J** and **K** defined in the previous sub-section.
In the current VFE scheme, the mass-weighted operators $\mathbf{G}^*$, $\mathbf{S}^*$ and $\mathbf{N}^*$ are defined as follows :

$$\mathbf{G}^* = (\mathbf{K}-\mathbf{J}).\mathbf{dL\Pi}^* \tag{17}$$

$$\mathbf{S}^* = (\mathbf{\Pi}^*)^{-1}.\mathbf{J}.\mathbf{d\Pi}^* \tag{18}$$

$$\mathbf{N}^* = (1/\pi_s^*)\mathbf{K}.\mathbf{d\Pi}^* \tag{19}$$

The non-dimensional SI linear operator $\mathbf{\Gamma}^*$ is defined by :

$$\mathbf{\Gamma}^* = (R/C_p)\mathbf{G}^*.\mathbf{S}^* + \mathbf{N}^* \tag{20}$$

The non-linear counterpart of these operators, **G**, **S** and **N** are defined as follows :

$$\mathbf{G} = (\mathbf{K} - \mathbf{J}).\mathbf{dL\Pi} \tag{21}$$
$$\mathbf{S} = \mathbf{\Pi}^{-1}.\mathbf{J}.\mathbf{d\Pi} \tag{22}$$
$$\mathbf{N} = (1/\pi_s)\mathbf{K}.\mathbf{d\Pi} \tag{23}$$

6 Principle of theoretical verifications for prescribed profiles $f(\eta)$

In order to check the accuracy of the discretisation, it may be convenient to compare the result of VFE integral operators applied to a prescribed profile with their continuous counterpart. This is always possible for the basic **J** operator, but not for the mass-weighted operators. This is generally not possible when the coordinate is only defined through a discrete set of values A, B and that the continuous laws used to defined these discrete A, B values are not known.
For general coordinates, when the analytical laws which defines A and B are known, it becomes in principle possible to compute the continuous mass-weighted integrals by replacing the mass-elements integrands by their analytic form and then integrate analytically.
The analytic computation of mass-weighted integrals is also possible in two other cases, even if the analytic laws used to define A and B are not known. The three cases where the evaluation is possible are discussed below.
It should be noted that for the verification against analytical results, we only consider functions f formulated in the physical coordinate η (hence more or less directly related to the hydrostatic pressure π) rather that functions formulated in terms of an unphysical continuous coordinate based on the level index, as e.g. defined by the coordinate x_l in (24) hereafter.

6.1 Case where A and B are analytically known

When A et B are analytically known, UH04's (3.2) can be extended to the continuous context as :

$$\eta(x_l) = A(x_l)/\pi_{00} + B(x_l) \tag{24}$$

where x_l is an independant continuous variable describing the interval $[0, L]$, in replacement of $\tilde{l}$. Then the height- and mass-elements π, $(d\pi/d\eta)$ and $(d\ln\pi/d\eta)$ can be directly deduced from the continuous equation :

$$\pi(\eta) = A(\eta) + B(\eta)\pi_s \tag{25}$$

where π_s is the surface pressure at the considered point. The knowledge of the profile $\eta(x_l)$ is required in order to define the values of the continuous height and mass elements knowing the value of π_s.

6.2 Case $\pi_s = \pi_{00}$

The computation of analytic integrals is possible for a general coordinate η when the effective surface pressure π_s is equal to the pressure π_{00} used in UH04's (3.1) to define the discrete values of η from the

discrete values of A and B. In this particular case UH04's (2.6) and (3.1) show that, in the continuous context :

$$\pi = \eta \pi_{00} \tag{26}$$

As a consequence, $(d\pi/d\eta) = \pi_{00}$ and $(d\ln\pi/d\eta) = (1/\eta)$. The expression of the continuous mass-weighted operators then simplifies into :

$$(\mathcal{G}X)_\eta = \int_\eta^1 \frac{X}{\eta'} d\eta' \tag{27}$$

$$(\mathcal{S}X)_\eta = \frac{1}{\eta}\int_{\eta_T}^\eta X d\eta' \tag{28}$$

$$(\mathcal{N}X)_\eta = \int_{\eta_T}^1 X d\eta' \tag{29}$$

which can be analytically computed for a prescribed function $X(\eta)$. It should be noted that it is possible to use these formulae even when $A_T \neq 0$ and/or $B_T \neq 0$.
This particular case $\pi_s = \pi_{00}$ allows to use any arbitrary coordinate, but is not very typical of the what occurs generally in the model, in which the surface pressure usually has significant variations. Using only this case for diagnostics could lead to an over-optimistic opinion since assuming $\pi_s = \pi_{00}$ acts in favour of the accuracy.

6.3 Case $A \equiv 0$

In this case, we have a pure σ coordinate. Insertion of $A = 0$ in UH04's (2.6) and (3.1) show that :

$$\pi = B\pi_s = \eta \pi_s \tag{30}$$

As a consequence, in the continuous context, $(d\pi/d\eta) = \pi_s$ and $(d\ln\pi/d\eta) = (1/\eta)$. The expression of the mass-weighted operators then simplifies into the same form as in the previous case. It should be noted that it remains possible to use these formulae even when $B_T \neq 0$.
This particular case $A \equiv 0$ allows to examine the behaviour of the mass-weighted operators for any value of the surface pressure, but it is restricted to particular coordinates. Using only this case for diagnostics could lead to an over-optimistic opinion since assuming $A \equiv 0$ eliminates the problems linked to the hybridicity of the coordinate.

*
* *

In this paper, evaluation of the response of operators on analytical profiles is performed for two coordinates : regular terrain-following coordinates (which satisfies the three above cases), and current ECMWF coordinate (hence only for the case $\pi_s = \pi_{00}$).

7 Possible avenues for the extension of the VFE to the NH model : hydrostatic operators

7.1 Constraint (C1)

In the current architecture of the NH model, the semi-implicit scheme is based on the algebraic elimination of all variables but one in the discrete context, in order to reach a single "discrete structure equation"

which is an Helmholtz equation solved in the spectral space. For this algebraic elimination to be possible, a mathematical constraint (C1) must be satisfied in the discrete context. This constraint (C1) writes :

$$-\mathbf{G}^*.\mathbf{S}^* + \mathbf{G}^* + \mathbf{S}^* - \mathbf{N}^* = 0 \tag{31}$$

The matrix $\mathbf{A_1} = -\mathbf{G}^*.\mathbf{S}^* + \mathbf{G}^* + \mathbf{S}^* - \mathbf{N}^*$ involved in the LHS of this equation must be identically zero. This constraint, which had be carefully taken into account for the FD discretisation of the NH model, has to be re-examined for the extension to the VFE discretisation.

Unfortunately, with the current version of the VFE discretisation, the matrix $\mathbf{A_1}$ is not found to be exactly zero. For the current $L = 60$ coordinate of the ECMWF, the maximum eigenvalue modulus of $\mathbf{A_1}$ is 0.107, to be compared to the maximum eigenvalues modules of $\mathbf{G}^*$ and $\mathbf{S}^*$, which are respectively 0.728 and 1. Therefore, it seems not very appropriate to use the set of integral operators directly derived from the hydrostatic VFE scheme for its extension to the NH model, because the constraint (C1) is not fulfilled. Using the operators as they are defined in the HPE model would result in imaginary eigenvalues of the discrete structure equation, and therefore, in an intrinsic instability of the linear model itself. Several solutions for fulfilling the constraint (C1) may be proposed. They are discussed and compared in the next subsections.

7.2 Modifying the architecture of the SI scheme

It can be seen from the documentation of the NH model (B. , 2004b) that the constraint (C1) arises because of the special architecture of ARPEGE's semi-implicit scheme : the constraint (C1) is necessary only because we want to be able to perform algebraically the elimination of all implicit variables but one. Yet, such a strategy is not absolutely necessary : in discrete form the implicit problem is just a linear inversion, and could be performed with two (or more) variables in the vector for which the SI operator is inverted. If we adopt a solution of the implicit problem for the couple (D,d), then the constraint (C1) does no longer need to be fulfilled, and the original operators $\mathbf{G}^*$, $\mathbf{S}^*$ and $\mathbf{N}^*$ can be used directly.
Technically, building the SI scheme on this strategy is probably not more difficult than with the current strategy. However, the design of such a scheme is a scientific issue, and we will try to avoid this avenue if possible because although changes would essentially be limited to the spectral part of the model, it breaks the continuity with the previous existing SI schemes in ARPEGE/IFS. If a more direct solution is possible and brings satisfaction, it should be preferred.

7.3 Modifying the operator $\mathbf{N}^*$

The simplest and the most natural idea to achieve the fulfilment of (C1) without modifying the structure of the SI scheme, would be to redefine the operator $\mathbf{N}^*$ specifically in this way. We would then define a new $\mathbf{N}'^*$ as :

$$\mathbf{N}'^* = \mathbf{G}^*.\mathbf{S}^* - \mathbf{G}^* - \mathbf{S}^* \tag{32}$$

However, this strategy has several disadvantages :

- With this definition, the $\mathbf{N}'^*$ operator has no special reason to remain constant-valued in the vertical, and indeed, it does not. Concretely, this means that the VFE total colum integral becomes level dependent ! This may look strange at first glance, but in fact this can be acceptable because the variations are quite weak : the VFE integral computed by $\mathbf{N}^*$ and $\mathbf{N}'^*$ are much closer mutually than they are to the analytic value. Fig. 2 shows an illustration of this fact : for the function

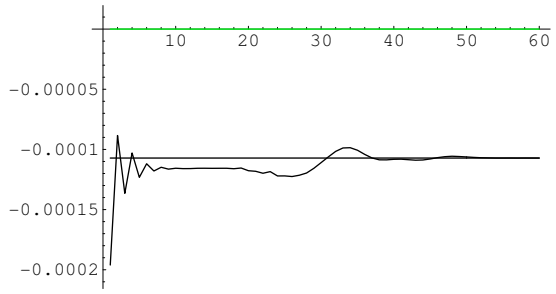

FIG. 2 – *Response of* $\mathbf{N}^*$ *(straight line) and* $\mathbf{N}'^*$ *operators for the function* $f(\eta) = \sin(6\pi\eta)$*, for the 60 levels discretisation of the ECMWF model. The analytical value is zero.*

$f(\eta) = \sin(6\pi\eta)$ and for the 60 current ECMWF level, the column integral by $\mathscr{N}^*$ is exactely zero, and the VFE values obtained with $\mathbf{N}^*$ and $\mathbf{N}'^*$ are very different from zero, but quite close together. From this point of view, the difference between the $\mathbf{N}'^*$ and $\mathbf{N}^*$ may be viewed as "inside" the noise-level, and although vertically non-constant, the error in $\mathbf{N}'^*$ is not significantly worse than the error of $\mathbf{N}^*$. Therefore, the level variability of $\mathbf{N}'^*$ is not a redhibitory argument against choosing it for fulfilling (C1).

- However, having a level-dependant result for $\mathbf{N}'^*$ means more or less than π_s becomes a 3D variable at least to some extent, and consequently needs some changes code to adapt to this new situation. In order to reduce this unpleasant consequence to a minimum, we could choose to restrict the 3D character of the π_s variable only to the linear SI system, which means that the RHS of the SI problem for the π_s equation would be 3D while the explicit equation for π_s would remain 2D. However the benefit of this restriction is quite small, because the spectral transform for π_s RHS still would have to remain 3D, and this means a deep reorganisation of the code, since spectral transforms is the most critical part of the relevant code to be changed.

This latter argument seems, in turn, quite a redhibitory one for a further examination of this strategy for fulfilling (C1), and this approach is thus abandoned here.

7.4 Modifying the operator $\mathbf{S}^*$

The equation :

$$\int_\eta^1 \frac{X(\eta')}{\eta'} d\eta' = X(\eta) \tag{33}$$

only admits the trivial solution $X(\eta) = 0$. As a consequence, the operator $(\mathscr{G}^* - \mathscr{I})$ is "inversible" in the sense that solving the integral equation :

$$(\mathscr{G}^* - \mathscr{I}).X(\eta) = f(\eta) \tag{34}$$

(where the unknown function is X and f is a prescribed function) leads to a single solution. For a given function f, the solution of (34) is :

$$X(\eta) = \frac{1}{\eta}\int_\eta^1 \left[\eta' \frac{df}{d\eta}(\eta')\right] d\eta' \; - \; \frac{f(1)}{\eta} \tag{35}$$

This property of the continuous operator $\mathscr{G}^*$ is well reflected by its VFE discrete counterpart : for $L = 60$ and a regular σ coordinate, the minimum eigenvalue modulus of $(\mathbf{G}^* - \mathbf{I})$ is 0.401 and the discrete operator $(\mathbf{G}^* - \mathbf{I})$ is therefore found to be inversible as in the continuous context.

Since the $(\mathbf{G}^* - \mathbf{I})$ operator is inversible, an solution for satisfying (C1) would be to redefine the $\mathbf{S}^*$ operator through the inversion of (C1). The resulting $\mathbf{S'}^*$ operator would thus write :

$$\mathbf{S'}^* = (\mathbf{G}^* - \mathbf{I})^{-1}.(\mathbf{G}^* - \mathbf{N}^*) \tag{36}$$

Using this approach allows π_s to remain a 2D variable, and thus it can be anticipated that only small changes in the code are required. Although the $\mathbf{\Gamma}^*$ operator is not used in the NH model, we define its modified version by using $\mathbf{S'}^*$ for subsequent verifications :

$$\mathbf{\Gamma}_{\mathbf{S'}}{}^* = (R/C_p)\mathbf{G}^*.\mathbf{S'}^* + \mathbf{N}^* \tag{37}$$

7.5 Modifying the operator $\mathbf{G}^*$

In the continuous context, the equation :

$$\frac{1}{\eta}\int_0^\eta X(\eta')d\eta' = X(\eta) \tag{38}$$

admits the non-trivial solution $X(\eta) = \text{Const}$. As a consequence, the operator $(\mathscr{S}^* - \mathscr{I})$ is "singular" in the sense that solving the integral equation $(\mathscr{S}^* - \mathscr{I}).X(\eta) = f(\eta)$ (with same conventions as in the previous subsection) leads to an infinity of solutions, mutually departing through a constant.
This property of the continuous operator $\mathscr{S}^*$ is well reflected by its VFE discrete counterpart : still for $L = 60$ and a regular σ coordinate, the minimum eigenvalue modulus of $(\mathbf{S}^* - \mathbf{I})$ is only $2.7\ 10^{-16}$, a value probably depending on the rounding errors in the computations. Although the discrete operator $(\mathbf{S}^* - \mathbf{I})$ is found inversible strictly speaking, (since the determinant is not exactly zero), the corresponding matrix is very badly conditioned and its extremely unaccurate inverse can not be used in practice. Therefore, a method for defining an operator $\mathbf{G'}^*$ by directly inverting (C1) as in (36) is not possible.
However, it should be noticed that $(\mathbf{S}^* - \mathbf{I})$ singular does not mean that there is no solution for $\mathbf{G'}^*$, but that the set of solutions $\mathbf{G'}^*$ satisfying (C1) is not reduced to one element. We can therefore determine $\mathbf{G'}^*$ as the operator which satisfies (C1) together with another arbitrary constraint (a "gauge" condition) to be determined, and which makes it physically meaningful.
A demonstration of the relevance of this approach in the continuous context is provided in the Appendix 1. This serves as a justification for applying the proposed strategy for determining an operator $\mathbf{G'}^*$ which satisfies (C1) and a gauge condition.

In the discrete context, we define the vector $\mathbf{1} = (1, \ldots, 1)$. and we use as a gauge condition :

$$\mathbf{G'}^*.\mathbf{1} = \mathbf{G}^*.\mathbf{1} \tag{39}$$

Therefore, when increasing the resolution, the $\mathbf{G'}^*$ will effectively converge toward its continuous counterpart, because it will converge toward the operator $\mathbf{G}^*$ which does. The operator $\mathbf{G'}^*$ that we seek can then be obtained by the simple following iterative process :

$$\mathbf{G}^{*(0)} = \mathbf{G}^* \tag{40}$$

$$\mathbf{G}^{*(i+1)} = \mathbf{G}^{*(i)}.\mathbf{S}^* - \mathbf{S}^* + \mathbf{N}^* \quad \text{for } i \geq 0 \tag{41}$$

and the iteration is stopped for a given $i_{\max}$ index, that is, $\mathbf{G}'^{*} = \mathbf{G}^{*(i_{\max})}$. Due to the correction of the mass elements [see (3) and (4)] we have, to the computer accuracy :

$$\mathbf{S}^{*}.\mathbf{1} = \mathbf{N}^{*}.\mathbf{1} = \mathbf{1} \tag{42}$$

Therefore :

$$\mathbf{G}^{*(i+1)}.\mathbf{1} = \mathbf{G}^{*(i)}.\mathbf{1} \tag{43}$$

consequently, any iterated $\mathbf{G}^{*(i)}$ satisfies the gauge condition, and so does also $\mathbf{G}'^{*}$.

Similarly to the previous subsection, a version of the operator $\mathbf{\Gamma}^{*}$ modified by using $\mathbf{G}'^{*}$ is defined for verifications :

$$\mathbf{\Gamma}_{\mathbf{G}'}{}^{*} = (R/C_p)\mathbf{G}'^{*}.\mathbf{S}^{*} + \mathbf{N}^{*} \tag{44}$$

7.6 Modified non-linear of operators G′, S′

The fulfilment of the constraint (C1) is, strictly speaking, required only for the SI linear integral operators. The non-linear operators could be left unmodified as they are defined in (21)–(23), or could be modified in the same way as the linear ones, in order to fulfil (C1) also in the explicit non-linear model. The benefit of choosing one or the other of these two approaches, or even another one, is not totally obvious, and these options should be examined as a future work.

First, it should be noticed that modifying $\mathbf{G}$ into $\mathbf{G}'$, or $\mathbf{S}$ into $\mathbf{S}'$ in the non-linear model to fulfill (C1) even for non-linear operators, induces a significant overcost in CPU and storage, and would need significant code reorganisations : for any value of the surface pressure (i.e. any column), a separate modified matrix would have to be computed through a complicated linear algebra process involving matrix inversions and matrix products, and possibly iterative. This contrasts with the current VFE scheme in which only a simple multiplication by a constant pre-calculated matrix is performed (via the subroutine `VERINT`). For this reason, it seems that computing a modified operator which fulfills (C1) in the non-linear model, even if technically possible and possibly beneficial, is not very realistic in terms of efficiency.

On the other hand, keeping the non-modified versions of non-linear operators is optimal for efficiency, but the discrepancy between the linear and non-linear operators may have detrimental consequences. For instance, if we use a terrain-following coordinate σ, we will loose the very nice property that for any value of the surface pressure, the non-linear operators are exactly identical to their linear counterpart, (see section 8.4). On contrary, for any value of the surface pressure, the non-linear operators will be different from their linear counterpart.

We propose a third intermediate method to define the non-linear operators : since the dependency on the surface pressure is achieved only through diagonal operators, we can define non-linear operators which converge to their linear counterpart for σ coordinates.

Modified G′ operator :

Returning to (17), the linear modified operator $\mathbf{G}'^{*}$ can be expressed as the product of the mass element $\mathbf{dL\Pi}^{*}$ by a modified upward basic vertical operator $(\mathbf{K}-\mathbf{J})'$ defined by :

$$(\mathbf{K}-\mathbf{J})' = \mathbf{G}'^{*}.[\mathbf{dL\Pi}^{*}]^{-1} \tag{45}$$

($\mathbf{dL\Pi}^{*}$ is always inversible by nature). Then the non-linear modified operator $\mathbf{G}'$ can be expressed as :

$$\mathbf{G}' = (\mathbf{K} - \mathbf{J})'.\mathbf{dL\Pi} \tag{46}$$

Modified $\mathbf{S}'$ operator :

Similarly, the linear modified operator $\mathbf{S}'^*$ can be expressed as the product of the mass elements $\mathbf{\Pi}^*$ and $\mathbf{d\Pi}^*$ by a modified downward basic vertical operator $\mathbf{J}'$ defined by :

$$\mathbf{J}' = \mathbf{\Pi}^*.\mathbf{S}'^*.[\mathbf{d\Pi}^*]^{-1} \tag{47}$$

($\mathbf{d\Pi}^*$ is also inversible by nature). Then the non-linear modified operator $\mathbf{S}'$ can be expressed as :

$$\mathbf{S}' = \mathbf{\Pi}^{-1}.\mathbf{J}'.\mathbf{d\Pi} \tag{48}$$

$$\overset{*}{*} \quad *$$

It can be seen that these modified non-linear operators $\mathbf{G}'$ and $\mathbf{S}'$ have no special reason to satisfy (C1) for a general value of π_s. In this respect, they are like the non-modified versions of these operators $\mathbf{G}$ and $\mathbf{S}$. However, they have the advantage on $\mathbf{G}$ and $\mathbf{S}$ that when π_s tends toward π_s^*, they converge toward their modified linear counterparts $\mathbf{G}'^*$ and $\mathbf{S}'^*$. Moreover, for σ coordinates $\mathbf{G}'$ and $\mathbf{S}'$ are exactly equal to their linear counterpart and therefore identically satisfy (C1). As a consequence, it can be seen that with this definition, $\mathbf{G}'$ and $\mathbf{S}'$ depart from their (C1)-fulfilling linear counterpart only to the extent that the actual coordinates depart from a terrain-following one, and then, only to the extent that the surface-pressure π_s departs from its reference counterpart π_s^*. Finally, one of the main advantages of this proposed approach, is that the operators $\mathbf{J}'$ or $(\mathbf{K} - \mathbf{J})'$ can be pre-computed and stored at the setup level, which makes the computation of $\mathbf{G}'$ or $\mathbf{S}'$ straightforward and efficient.

8 Behaviour of current and proposed VFE schemes for regularly spaced σ coordinates

In this section we examine the behaviour of the VFE scheme implemented in the IFS code and of the proposed avenues for NH, in the context of a regularly spaced terrain-following coordinate. This examination mainly involves the aspects linked to the accuracy and normal modes of the scheme. A general terrain-following σ coordinate is defined by $A \equiv 0$. Hence for a σ coordinate, all aspects linked to A become trivial and will not be discussed further in this section.

In the case where the formal description $\eta = A/\pi_{00} + B$ is used (as in UH04), a regularly spaced σ coordinate means that in addition to $A \equiv 0$, we have $B(x_l) \equiv \eta(x_l) \equiv (x_l/L)$, where x_l is the continuous coordinate defined by (24). As a consequence, for a regularly spaced σ coordinate with the UH04 formal description, we have :

$$A_{\widetilde{l}} = 0 \tag{49}$$

$$B_{\widetilde{l}} = (\widetilde{l}/L) \tag{50}$$

for $0 \leq \widetilde{l} \leq L$.

8.1 Accuracy of the K operator on the function $f(\eta) = 1$

For a continuous σ coordinate, the factor $(\partial B/\partial \eta)$ appearing in UH04's (2.9) simply writes :

$$\frac{\partial B}{\partial \eta} = 1 \tag{51}$$

The normalisation in (2) therefore simply involves the VFE total column integral of the uniform function $f(\eta) = 1$. The analytical and the FD values for this integral are obviously 1 for a σ coordinate.
The Fig. 3 depicts the variations of the departure of the integral with respect to 1 for various values of L. The departure from the analytical value is found small in the case of a regular σ coordinate, the error being of the order of 10^{-8} in any cases.

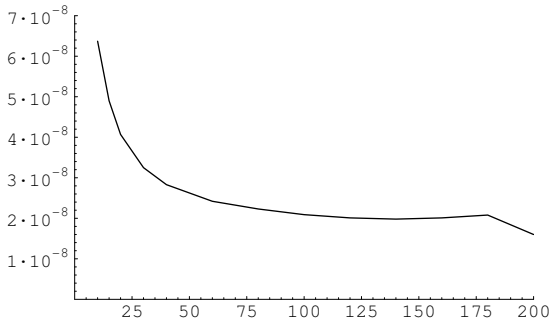

FIG. 3 – *Values of the error of the total column VFE integral of the function $f(\eta) = 1$ for a regularly spaced σ coordinate with various values of L in [10, 200]*

8.2 Accuracy of the derivative of the J operator on the analytic function $f(\eta) = \sin(6\pi\eta)$

The response of the FD derivative of the integral operator **J** for a prescribed analytic function $f(\eta) = \sin(6\pi\eta)$ is examined in UH04 for a 60 levels regular σ discretisation. The results are given in the Table 1 of UH04, but we did not succeed to reproduce them exactly. The results are given here in a more suggestive graphical form.
The "FD-fashion" vertical derivative of the analytic integral and of the VFE integral are plotted in Fig. 4 , as well as the absolute error which is the difference between the two latter curves. The analytic and VFE curves (thin solid lines) are almost undistiguishable. For clarity, the absolute error (thick dashed line) is enlarged by a factor of 100.

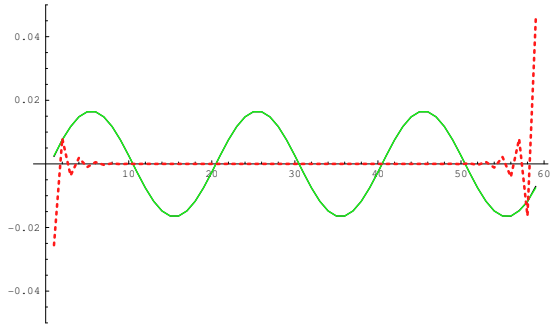

FIG. 4 – *Analytic and VFE values of the "FD-fashion" derivative of the integral of the function $f(\eta) = \sin(6\pi\eta)$ (solid lines) for a regular σ coordinate with $L = 60$. Absolute error multiplied by 100 (thick dashed line).*

The same figure is plotted in the same format for the FD discretisation of the integral operator in Fig. 5. The FD counterpart of the **J** integral operator is not defined in the model but it can be defined in a standard way by :

$$(\mathbf{J}.X)_l = (\eta_l - \eta_{\widetilde{l-1}})X_l + \sum_{k=1}^{l-1}(\eta_{\widetilde{k}} - \eta_{\widetilde{k-1}})X_k \tag{52}$$

The magnitude of the error is uniformly larger for the FD operator, except near the two edges, where the VFE discretisation results in bigger errors. The two thin solid lines are very slightly distinguishable near the extrema of the curves of the FD response.

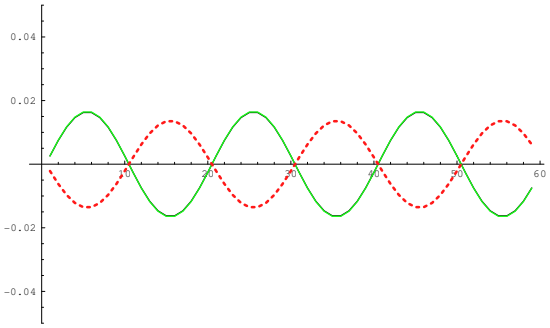

FIG. 5 – *Analytic and FD values of the "FD-fashion" derivative of the integral of the function* $f(\eta) = \sin(6\pi\eta)$ *(solid lines) for a regular* σ *coordinate with* $L = 60$*. Absolute error multiplied by 100 (thick dashed line).*

As outlined in Table 1 of UH04, the error is very small in the central part of the domain for the VFE scheme. Similar results are found here : the mean magnitude of the absolute error in the interval [20,40] is $2.76\ 10^{-10}$ for the VFE scheme, while for the FD scheme it is $8.43\ 10^{-5}$, that is, five order of magnitude bigger.

8.3 Accuracy of the J operator on the analytic function $f(\eta) = \sin(6\pi\eta)$

The behaviour of the operator **J** is now diagnosed directly, and not through its FD derivative as in the previous subsection. The VFE and analytic values are superimposed in the left panel of Fig. 6, while the error of the VFE values multiplied by a factor of 100 is displayed in the right panel. The error level is found significant, although almost uniform, which justifies the good results see in the previous subsection.

The results are shown in the same format in Fig. 7, for the standard FD vertical integral operator. The level of the error is found of comparable magnitude than for the VFE scheme. It seems that the benefit of the VFE scheme is rather to produce an error that is constant with height rather than a small error in an absolute sense. The practical meaning of this latter remark is however not very clear for the author. In particular, it is not very clear if the presentation of the results in the shape of the previous subsection only is susceptible or not to give an over-optimistic picture of the quality of the VFE scheme compared to the FD scheme.

8.4 Mass-weighted operators in σ coordinates

For a (regular or stretched) σ coordinate, the linear operators mass-weighted operators and their non-linear counterpart are identical :

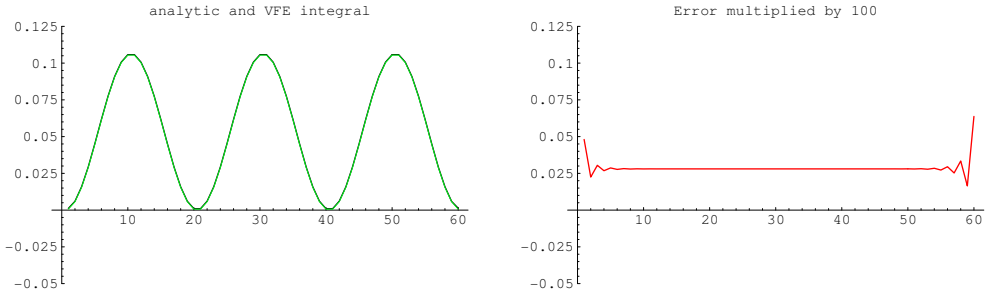

FIG. 6 – *Analytic and VFE values of the* **J** *operator for the function* $f(\eta) = \sin(6\pi\eta)$ *(left) for a regular* σ *coordinate with* $L = 60$. *Absolute error multiplied by 100 (right).*

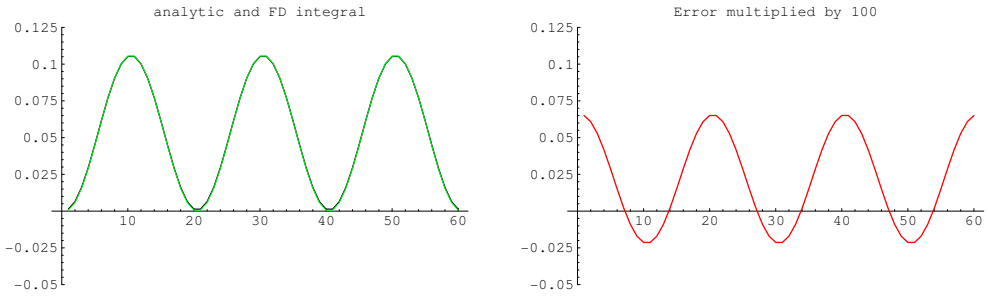

FIG. 7 – *Analytic and FD values of the* **J** *operator for the function* $f(\eta) = \sin(6\pi\eta)$ *(left) for a regular* σ *coordinate with* $L = 60$. *Absolute error multiplied by 100 (right).*

$$\mathscr{G} = \mathscr{G}^* \tag{53}$$
$$\mathscr{S} = \mathscr{S}^* \tag{54}$$
$$\mathscr{N} = \mathscr{N}^* \tag{55}$$

and these operators write :

$$(\mathscr{G}X)_\sigma = \int_\sigma^1 \frac{X}{\sigma'} d\sigma' \tag{56}$$
$$(\mathscr{S}X)_\sigma = \frac{1}{\sigma}\int_0^\sigma X d\sigma' \tag{57}$$
$$(\mathscr{N}X)_\sigma = \int_0^1 X d\sigma' \tag{58}$$

Similar formulae apply for discrete operators **G**, **S** and **N** for the non-modified operators :

$$\mathbf{G} = \mathbf{G}^* \tag{59}$$

$$\mathbf{S} = \mathbf{S}^* \tag{60}$$

$$\mathbf{N} = \mathbf{N}^* \tag{61}$$

Similar properties hold for modified operators ($\mathbf{G}' = \mathbf{G}'^*$ or $\mathbf{S}' = \mathbf{S}'^*$) only if the non-linear operators are also modified, as proposed above. Since we assume that non-linear operators are modified, the examination of both nonlinear and linear operators is not necessary, and it is sufficient to present the results only for the linear operators in this section devoted to the pure regular σ coordinate.

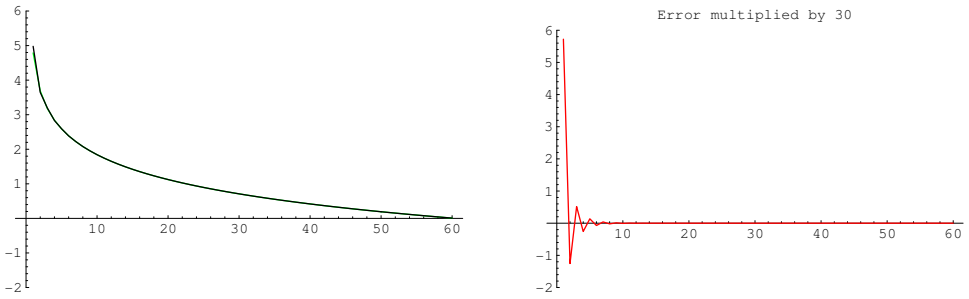

FIG. 8 – *Analytic and VFE values of the* $\mathbf{G}^*$ *operator for the function* $f(\eta) = 1$ *(left) for a regular* σ *coordinate with* $L = 60$*. Absolute error multiplied by 30 (right).*

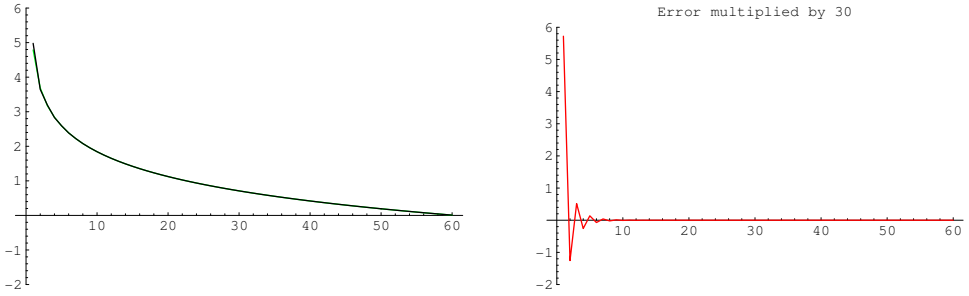

FIG. 9 – *Analytic and VFE values of the* $\mathbf{G}'^*$ *operator for the function* $f(\eta) = 1$ *(left) for a regular* σ *coordinate with* $L = 60$*. Absolute error multiplied by 30 (right).*

8.5 Accuracy of operators $\mathbf{G}^*$, $\mathbf{G}'^*$ on the function $f(\eta) = 1$

Still for a regular σ coordinate with $L = 60$, the behaviour of the $\mathbf{G}^*$ operator applied to the function $f(\eta) = 1$ is depicted in Fig. 8. The left panel shows the analytic and VFE integrals, and the right panel shows the error multiplied by a factor of 30. The results for the operator $\mathbf{G}'^*$ are depicted in Fig. 9 in the same format.

As expected, the responses of $\mathbf{G}^*$ and $\mathbf{G}'^*$ operators are identical for the function $f(\eta) = 1$, since this is precisely the gauge condition that we have employed in order to uniquely specify $\mathbf{G}'^*$. The level of the error is quite large for this vector, with a maximum magnitude of about 0.2 at the top.

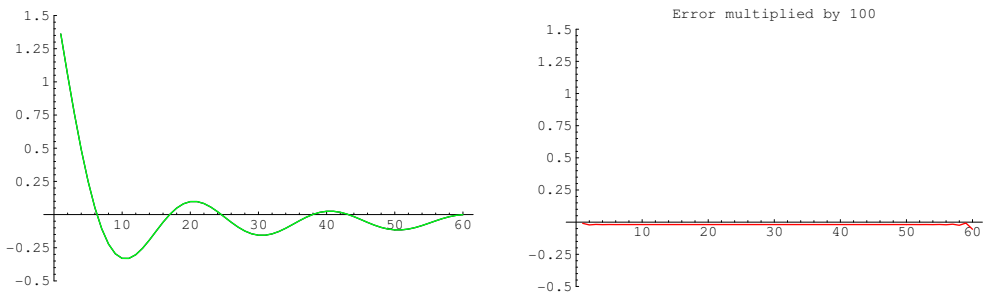

FIG. 10 – *Analytic and VFE values of the* $\mathbf{G}^*$ *operator for the function* $f(\eta) = \sin(6\pi\eta)$ *(left) for a regular* σ *coordinate with* $L = 60$*. Absolute error multiplied by 100 (right).*

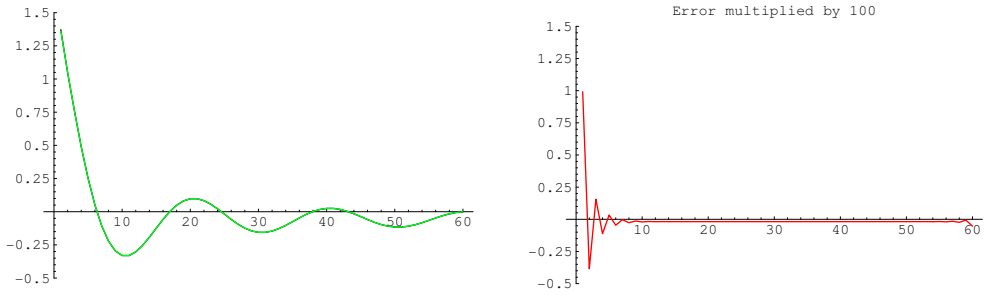

FIG. 11 – *Analytic and VFE values of the* $\mathbf{G}'^*$ *operator for the function* $f(\eta) = \sin(6\pi\eta)$ *(left) for a regular* σ *coordinate with* $L = 60$*. Absolute error multiplied by 100 (right).*

8.6 Accuracy of operators $\mathbf{G}^*$, $\mathbf{G}'^*$ on the function $f(\eta) = \sin(6\pi\eta)$

The comparison of operators $\mathbf{G}^*$ and $\mathbf{G}'^*$ is now shown for the function $f(\eta) = \sin(6\pi\eta)$ in Figs. 10 and 11, in the same format as previously (the errors are multplied by a factor of 100). For the operator $\mathbf{G}^*$, it is seen that the magnitude of the error is much smaller than in the previous test (maximum magnitude about 0.0005). For $\mathbf{G}'^*$, there are still large values of the error near the very top of the domain, but their magnitude (about 0.01) is less than for the "external" mode $f(\eta) = 1$ examined previously. Inside the domain, the error of the two operators is similar (about 0.0002).
For comparison, the response of the operator $\mathbf{G}^*$ in the FD discretisation is plotted in Fig. 12. The VFE discretisation of $\mathbf{G}^*$ and $\mathbf{G}'^*$ appears to be more accurate than the FD discretisation, particularly inside the domain.

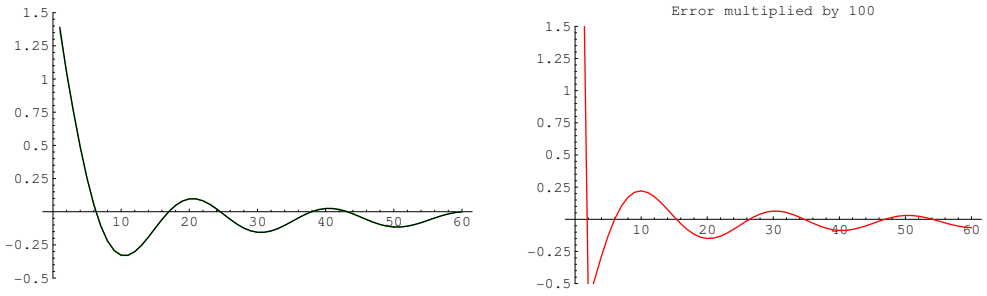

FIG. 12 – *Analytic and FD values of the* $\mathbf{G}^*$ *operator for the function* $f(\eta) = \sin(6\pi\eta)$ *(left) for a regular* σ *coordinate with* $L = 60$*. Absolute error multiplied by 100 (right).*

8.7 Accuracy of $\mathbf{S}^*$, $\mathbf{S}'^*$ on the function $f(\eta) = 1$

Due to (42), we have $\mathbf{S}^*.\mathbf{1} = \mathbf{1}$ and the error is zero to the computer accuracy for this test (figure not shown). Eq. (42) also implies :

$$\mathbf{S}'^*.\mathbf{1} = (\mathbf{G}^* - \mathbf{I})^{-1}.(\mathbf{G}^* - \mathbf{N}^*).\mathbf{1} = (\mathbf{G}^* - \mathbf{I})^{-1}.(\mathbf{G}^* - \mathbf{I}).\mathbf{1} = \mathbf{1} \tag{62}$$

and therefore, both $\mathbf{S}^*$ and $\mathbf{S}'^*$ have no error when applied to this vector.

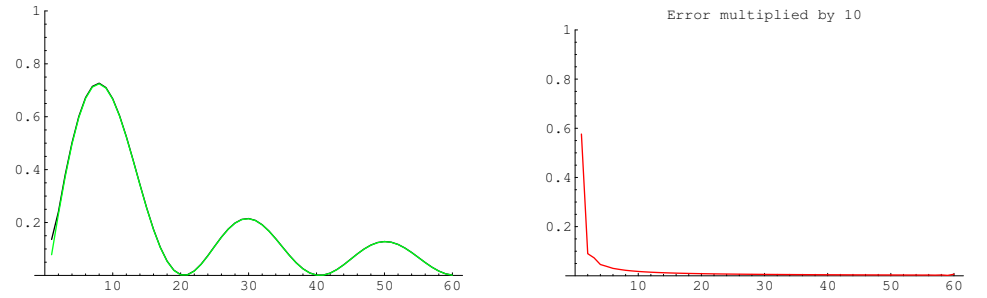

FIG. 13 – *Analytic and VFE values of the* $\mathbf{S}^*$ *operator for the function* $f(\eta) = \sin(6\pi\eta)$ *(left) for a regular* σ *coordinate with* $L = 60$*. Absolute error multiplied by 10 (right).*

8.8 Accuracy of $\mathbf{S}^*$, $\mathbf{S}'^*$ on the function $f(\eta) = \sin(6\pi\eta)$

The analytical value of $(\mathbf{S}^*)$ and its VFE counterpart are depicted in Fig. 13 (left panel) for the function $f(\eta) = \sin(6\pi\eta)$. The error is depicted on the right panel, multiplied by a factor of 10. The maximum error is located near the top of the domain, where the analytical and discrete curves slightly depart visually in the left panel.

The same fields are depicted in Fig. 14, but for the operator $\mathbf{S}'^*$. The error appears to be of similar magnitude, except near the top, where the magnitude is twice bigger.

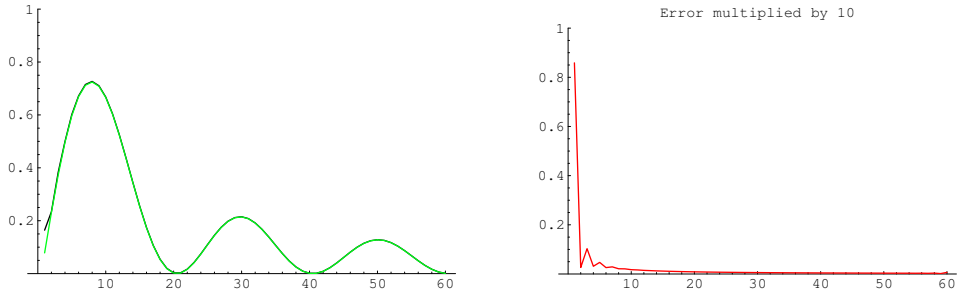

FIG. 14 – *Analytic and VFE values of the* $\mathbf{S}'^{*}$ *operator for the function* $f(\eta) = \sin(6\pi\eta)$ *(left) for a regular* σ *coordinate with* $L = 60$*. Absolute error multiplied by 10 (right).*

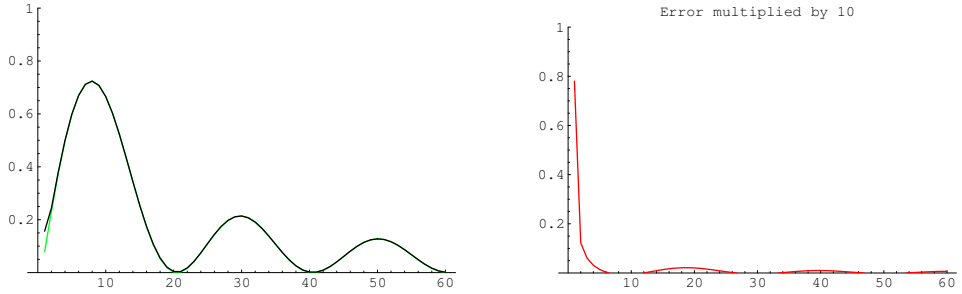

FIG. 15 – *Analytic and FD values of the* $\mathbf{S}^{*}$ *operator for the function* $f(\eta) = \sin(6\pi\eta)$ *(left) for a regular* σ *coordinate with* $L = 60$*. Absolute error multiplied by 10 (right).*

For comparisons, the same fields are depicted in Fig. 15, but for the FD version of the operator $\mathbf{S}^{*}$. Here, in opposition to the previous results for the $\mathbf{G}^{*}$ operator, the error appears here to be of similar magnitude than for the VFE operators.

8.9 Eigenvalues and eigenmodes of mass-weighted operators

The examination of the eigenmodes of $\mathbf{S}^{*}$ or $\mathbf{G}^{*}$ seems to be not very interesting because the eigenspaces of the continuous counterparts of these operators are very vast. These individual operators are not directly involved in modes propagation and thus their eigenmodes have no immediate physical meaning.

On the other hand, the eigenmodes of the $\mathbf{\Gamma}^{*}$ operator have a physical meaning, at least for the HPE model. However, the study of the eigenmodes of these operators is not very interesting in view of the NH model, because the normal modes of the NH model are given by those of the vertical Laplacian operator and not by those of $\mathbf{\Gamma}^{*}$. Nevertheless, for the completeness of the information, the eigenmodes of $\mathbf{\Gamma}^{*}$, $\mathbf{\Gamma}^{*}_{\mathbf{S}'}$ and $\mathbf{\Gamma}^{*}_{\mathbf{G}'}$ are presented here.

The eigenmodes of the continuous counterpart of $\mathbf{\Gamma}^{*}$, can be computed directly. They write :

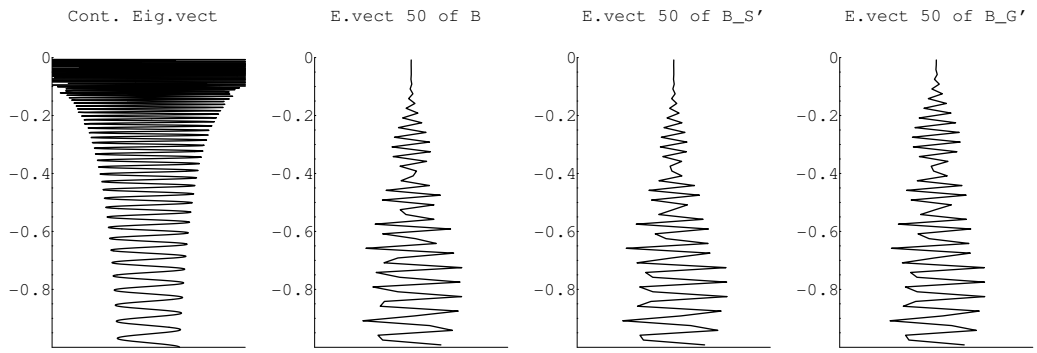

FIG. 16 – *Eigenvectors of* $\mathbf{\Gamma}^*$, $\mathbf{\Gamma}^*_{\mathbf{S}'}$ *and* $\mathbf{\Gamma}^*_{\mathbf{G}'}$ *operators for the mode number 50, for a regular* σ *coordinate with* $L = 60$.

$$X(\sigma) = X_0 \sigma^{-1/2} \left[\nu \cos(i\nu \ln \sigma) - \frac{C_v - R}{C_p} \sin(i\nu \ln \sigma) \right] \quad \text{with } X_0 \in \mathbb{R} \text{ and } \nu \in \mathbb{R}^+ \tag{63}$$

The eigenvalue associated to the eigenmode with ν in the above formula is :

$$\lambda = \frac{R}{C_p} \frac{1}{\nu^2 + 1/4} \tag{64}$$

The continuous and the discrete eigenvectors of $\mathbf{\Gamma}^*$, $\mathbf{\Gamma}^*_{\mathbf{S}'}$ and $\mathbf{\Gamma}^*_{\mathbf{G}'}$ are shown in Fig. 16 for the discrete mode number 50. The continuous mode has been chosen so to have roughly the same wavelength at the bottom of the domain, where it is well resolved. The vertical wavelength of the continuous normal mode in σ coordinate decreases toward zero with height, while its magnitude increases due to the decrease of density with height.

It is seen that when the vertical resolution becomes insufficient, the amplitude of discrete modes vanishes, which means that the mode is no longer described in this area. This behaviour is characteristic of variable-resolution systems : it means that when a component penetrates in an area with a mesh poorer than its wavelength, this component is subjected to a complete internal reflection toward the well-resolved area. Compared to the continuous behaviour, such a normal-mode structure therefore means that a false reflection occurs at this location. It must be outlined that other discretisations may have another "reaction" with respect to the problem of impinging component into a non-resolved area : it is sometimes observed that the modes are not vanishing in the non-resolved area. This, in turn, means that an impinging component will be transmitted in the non-resolved area, but with the smallest resolved wavelength, that is, it will be transmitted in a distorted fashion. We see that variable resolution models are doomed to suffer from either false internal reflection, or erroneously distorted transmission when waves are impinging into a non-resolved area. The author does not want to express his support for one of these two drawbacks or for the other. An example of erroneous distorted transmission can be seen for the vertical modes of the finite difference discretisation, in UH04' Figs. 6 and 7.

Nevertheles, for the depicted mode index, there are no dramatic differences in the vertical structure of the eigenvectors between the operators $\mathbf{\Gamma}^*$, $\mathbf{\Gamma}^*_{\mathbf{S}'}$ and $\mathbf{\Gamma}^*_{\mathbf{G}'}$. The same result holds for other mode indexes (not shown).

An noticeable feature is that whilst $\mathbf{\Gamma}^*_{\mathbf{G}'}$ and $\mathbf{\Gamma}^*$ have real positive spectra, the operator $\mathbf{\Gamma}^*_{\mathbf{S}'}$ exhibits complex eigenvalues. This means that $\mathbf{S}'^*$ could not be used for the HPE model because of the instability of the linear system. The instability is found be weak : the maximum imaginary part is 10^{-7} and the maximum eigenvalue is 1.38. However, the $\mathbf{\Gamma}^*$ operator is not used in the NH model, and the complexity of the spectrum of $\mathbf{\Gamma}^*_{\mathbf{S}'}$ is not redhibitory in itself.

9 Behaviour of current and proposed VFE schemes with NWP-type coordinates

The study of the behaviour of the VFE for regular σ coordinates is relevant in order to understand the theoretical properties of the scheme, but is also restrictive in the sense that these coordinates do not reflect well the kind of coordinates used in NWP models. Hence, we focus in this section on the behaviour of the scheme for the current disposition of the 60 hybrid-coordinate levels of the ECMWF discretisation. As mentionned above, since the analytical description of the coordinate is not known, the comparison of vertical operators to their analytical counterpart is possible only in the case where $\pi_s = \pi_{00}$. This latter condition is therefore assumed in the remaining of this section.

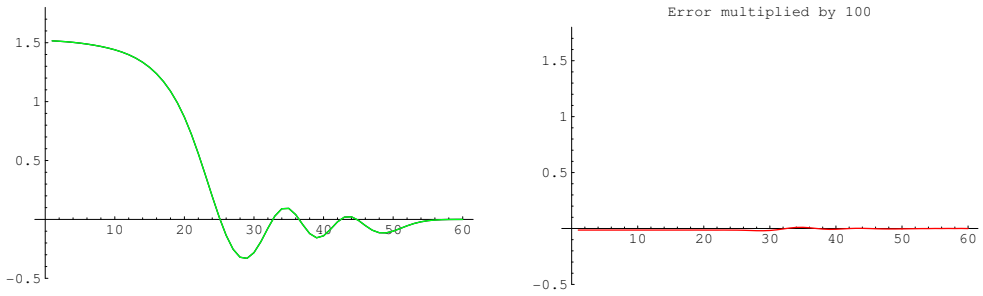

FIG. 17 – *Analytic and VFE values of the* $\mathbf{G}^*$ *operator for the function* $f(\eta) = \sin(6\pi\eta)$ *(left) for the ECMWF coordinate with* $L = 60$*. Absolute error multiplied by 100 (right).*

9.1 Accuracy of $\mathbf{G}^*$, $\mathbf{G}'^*$ on the function $f(\eta) = \sin(6\pi\eta)$

The response of the operators $\mathbf{G}^*$, $\mathbf{G}'^*$ for the function $f(\eta) = \sin(6\pi\eta)$ are depicted in Figs. 17 and 18 respectively. The errors are multiplied by a factor of 100. The error exhibits a very similar structure and magnitude. For comparison, the response of the FD version of the $\mathbf{G}^*$ operator is depicted in Fig. 19. The error is much bigger than for the VFE operators.

9.2 Accuracy of $\mathbf{S}^*$, $\mathbf{S}'^*$ on the function $f(\eta) = \sin(6\pi\eta)$

The response of the operators $\mathbf{S}^*$, $\mathbf{S}'^*$ for the function $f(\eta) = \sin(6\pi\eta)$ are depicted in Figs. 20 and 21 respectively. The errors are multiplied by a factor of 10. The error for $\mathbf{S}'^*$ has a larger magnitude than for $\mathbf{S}^*$ near the top. For comparison, the response of the FD version of the $\mathbf{S}^*$ operator is depicted in Fig. 22. The error is much bigger than for both of the previous VFE operators in the inner domain, however, it should be noted that the magnitude of the error near the top is much smaller than for VFE operators.

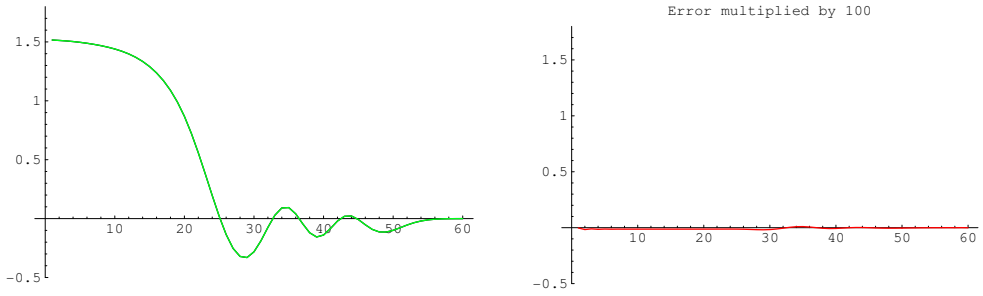

FIG. 18 – *Analytic and VFE values of the* $\mathbf{G}'^{*}$ *operator for the function* $f(\eta) = \sin(6\pi\eta)$ *(left) for the ECMWF coordinate with* $L = 60$*. Absolute error multiplied by 100 (right).*

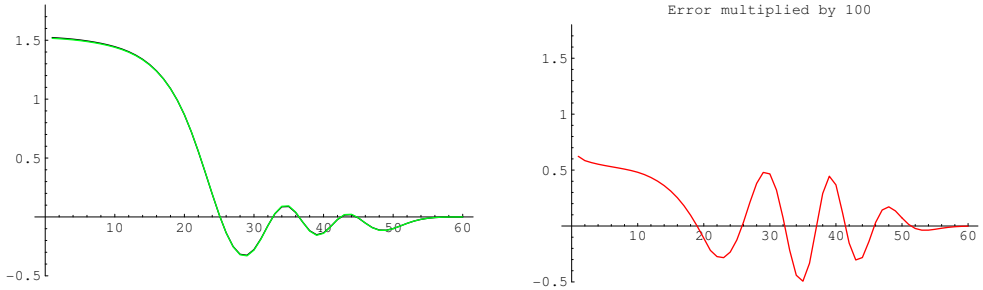

FIG. 19 – *Analytic and FD values of the* $\mathbf{G}^{*}$ *operator for the function* $f(\eta) = \sin(6\pi\eta)$ *(left) for the ECMWF coordinate with* $L = 60$*. Absolute error multiplied by 100 (right).*

9.3 Eigenmodes of mass-weighted operators

The structure of the eigenvector with the mode index 50 is depicted in Fig. 23 for the analytic operator and for the VFE operators $\mathbf{\Gamma}^{*}$, $\mathbf{\Gamma}^{*}_{\mathbf{S}'}$ and $\mathbf{\Gamma}^{*}_{\mathbf{G}'}$. In opposition to the results obtained with a regular σ coordinate, the modes for the operator $\mathbf{\Gamma}^{*}_{\mathbf{G}'}$ appear to be significantly different from the modes of $\mathbf{\Gamma}^{*}$ and $\mathbf{\Gamma}^{*}_{\mathbf{S}'}$. The amplitude of the mode does no longer vanish in the not-resolved part of the domain, but on contrary increases dramatically. This behaviour is similar to the one observed with the FD Lorenz discretisation, and its "physical" meaning has been discussed above.

As for the regular σ coordinate, it is noticeable that the spectrum of the $\mathbf{\Gamma}^{*}_{\mathbf{S}'}$ operator is found to be complex. The resulting instability for a use in a HPE model is probably still weak, since the maximum eigenvalue imaginary part is 0.0001 while the maximum eigenvalue of the operator is 1.40. Once again this feature is not redhibitory in itself for the use in the NH model.

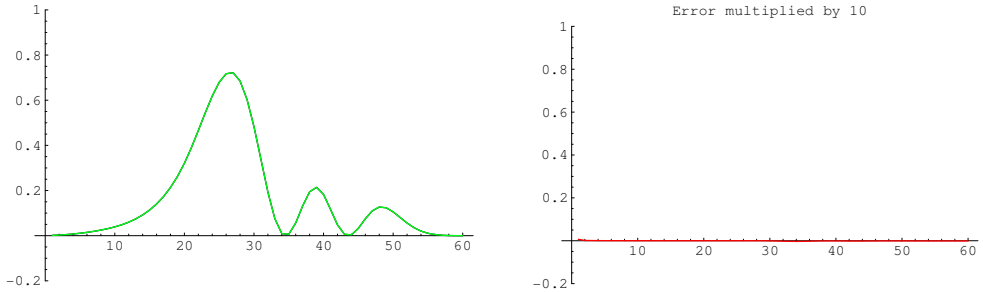

FIG. 20 – *Analytic and VFE values of the* $\mathbf{S}^*$ *operator for the function* $f(\eta) = \sin(6\pi\eta)$ *(left) for the ECMWF coordinate with* $L = 60$*. Absolute error multiplied by 10 (right).*

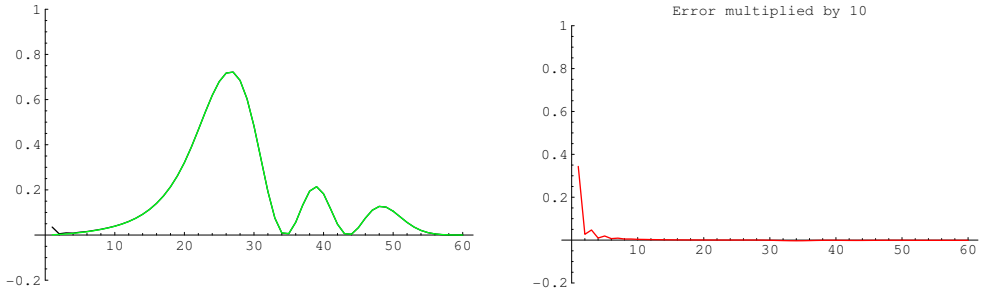

FIG. 21 – *Analytic and VFE values of the* $\mathbf{S}'^*$ *operator for the function* $f(\eta) = \sin(6\pi\eta)$ *(left) for the ECMWF coordinate with* $L = 60$*. Absolute error multiplied by 10 (right).*

9.4 Synthesis of sections 8 and 9

The design of the NH SI version in its current general design imposes the fulfilment of the constraint (C1). Since a general redefinition of the solution of the implicit problem and the use of a modified $\mathbf{N}'^*$ operators have been eliminated, a choice between the use of the modified $\mathbf{G}'^*$ and $\mathbf{S}'^*$ must be made.

For NWP-type coordinates, the accuracy of the modified $\mathbf{G}'^*$ operator seems to be very close from the one of the original operator $\mathbf{G}^*$. The relative accuracy of $\mathbf{G}'^*$ compared to $\mathbf{G}^*$ is slightly worse for regular coordinates, but in any case $\mathbf{G}'^*$ is much closer from $\mathbf{G}^*$ than from its FD counterpart. The spectrum of the HPE SI operator $\mathbf{\Gamma}^*_{\mathbf{G}'}$ obtained using $\mathbf{G}'^*$ is very similar to its original counterpart $\mathbf{\Gamma}^*$. The vertical structure of the eigenmodes of the $\mathbf{\Gamma}^*_{\mathbf{G}'}$ operator is not vanishing in non-resolved areas, however, this feature should not be detrimental in practice for the NH model since the normal modes of the NH model are not related to those of the $\mathbf{\Gamma}^*_{\mathbf{G}'}$ operator but to those of the vertical Laplacian operator $\mathbf{L}^*$ (defined below).

For regular and for NWP-type coordinates, the relative accuracy of the $\mathbf{S}'^*$ operator compared to the one of $\mathbf{S}^*$ seems to be roughly the same as for the $\mathbf{G}$ operators examined above. The structure of the eigenmodes of $\mathbf{\Gamma}^*$ and $\mathbf{\Gamma}^*_{\mathbf{S}'}$ is very similar, but the spectrum of $\mathbf{\Gamma}^*_{\mathbf{S}'}$ contains complex eigenvalues. However,

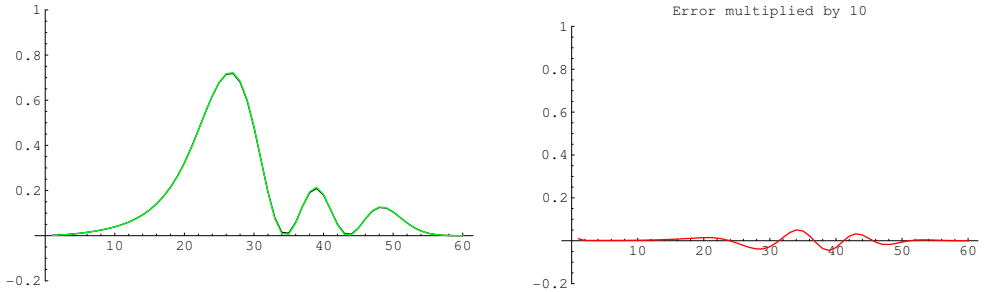

FIG. 22 – *Analytic and FD values of the* $\mathbf{S}^*$ *operator for the function* $f(\eta) = \sin(6\pi\eta)$ *(left) for the ECMWF coordinate with* $L = 60$*. Absolute error multiplied by 10 (right).*

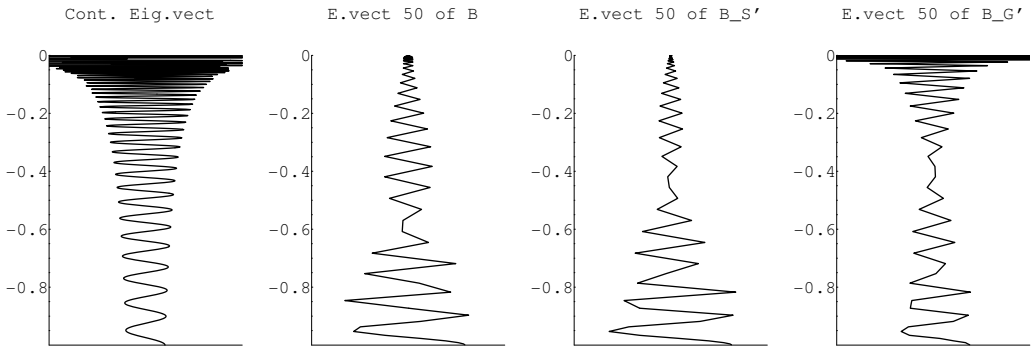

FIG. 23 – *Eigenvectors of* $\mathbf{\Gamma}^*$, $\mathbf{\Gamma}^*_{\mathbf{S}'}$ *and* $\mathbf{\Gamma}^*_{\mathbf{G}'}$ *operators for the mode number 50, for the current ECMWF coordinate with* $L = 60$*.*

this latter feature should not be detrimental in practice for similar reasons as above.

Finally, at this stage the relative advantage of choosing $\mathbf{G}'^*$ or $\mathbf{S}'^*$ as modified operator to fulfill the constraint (C1) is not very clear and they will be kept as potential candidates in the following. However, it is clear that these modified operators are not convenient for HPE modelling because they lead to either unstable eigenmodes (for $\mathbf{S}'^*$), or to noisy eigenmodes near the top (for $\mathbf{G}'^*$).

10 Possible avenues for the extension of the VFE to the NH model : non-hydrostatic operators

10.1 Constraint (C2)

In the NH model, in addition to the classical vertical integral operators already present in the HPE model, a so-called vertical "Laplacian" appears in the equation of the vertical momentum. This operator is applied to the nonhydrostatic pressure departure.

When forming the Helmholtz structure equation in the semi-implicit scheme of the NH model, a constraint appears in addition to the constraint (C1) encountered previously. The new constraint (C2) links this vertical "Laplacian" operator to the mass-weighted vertical operators. In the continuous case, this constraint (C2) is an identity which writes :

$$\mathscr{L}.\left[\mathscr{S}.\mathscr{G}-\frac{C_p}{C_v}(\mathscr{S}+\mathscr{G})\right]=\left(\frac{R}{C_v}\right)\mathscr{I} \tag{65}$$

where $\mathscr{L}$ is the vertical so-called "Laplacian" operator defined by :

$$\mathscr{L}.X=\left(1+\pi\frac{\partial}{\partial\pi}\right)\left(\pi\frac{\partial X}{\partial\pi}\right) \tag{66}$$

In the discrete context, this constraint (C2) writes :

$$\mathbf{L}^*.\left[\mathbf{S}^*.\mathbf{G}^*-\frac{C_p}{C_v}(\mathbf{S}^*+\mathbf{G}^*)\right]\equiv\mathbf{L}^*.\mathbf{A}_2^*=\left(\frac{R}{C_v}\right)\mathbf{I} \tag{67}$$

However, it is important to note that in opposition to (C1), the constraint (C2) does not need to be fulfilled exactly. The reason is that this constraint is not directly involved in the algebraic feasability of the SI scheme. The SI scheme of the NH model can perfectly be built even if (C2) is not fulfilled, or "partly" fulfilled. In this sense, the constraint (C2) is weaker than the constraint (C1). Since the constraint (C2) is not absolutely necessary, it can be "degenerated" into weaker properties that are interesting to be fulfilled even if the full constraint is not exactly fulfilled. The minimal sub-property of (C2) that should be fulfilled in any case is :

(C'2) : $\mathbf{L}^*.\mathbf{A}_2^*$ has only real positive eigenvalues

If this property was not fullfilled, the space-discretised structure equation would have complex or negative coefficients for some eigenmodes, and hence, these eigenmodes would be exponentially growing with time.

In a practical way, once the mass-weighted hydrostatic integral operators are chosen, the constraint (C2) acts on the choice of the discrete "Laplacian" operator $\mathbf{L}^*$. However, the main difficulty is that $\mathbf{L}^*$ must be defined in such a way that both $-\mathbf{L}^*$ and $\mathbf{L}^*.\mathbf{A}_2^*$ have purely real and positive spectra. Otherwise the linear model itself will become unstable, because it will have normal modes with complex frequencies. Several types of strategies can then be examined with respect to (C2) :

(i) Define the $\mathbf{L}^*$ operator in a pure VFE fashion, virtually ignoring the constraint (C2). The main risk is then that the minimal sub-constraint (C'2) is not fulfilled.

(ii) Define the discrete "Laplacian" operator directly from operators $\mathbf{G}^*$, $\mathbf{S}^*$ in order that (C2) is exactly fulfilled. In this case $\mathbf{L}^*$ is simply defined by inverting (C2).

(iii) Define the $\mathbf{L}^*$ operator in a pure FD fashion, virtually ignoring the constraint (C2). The risk is then that the minimal sub-constraint (C'2) is not fulfilled.

(iv) Define the discrete "Laplacian" operator independently of operators $\mathbf{G}^*$, $\mathbf{S}^*$, but in such a way that (C'2) is fulfilled.

(v) other unexplored options...

10.2 Defining the $\mathbf{L}^*$ operator in a pure VFE fashion

In this option, a VFE approach as in UH04 would be chosen to define the operator $\mathbf{L}^*$ from a pure mathematically-based VFE fashion. This is expected to result in an optimal accuracy for the discrete model. However, there is no guarantee that the sub-constraint (C'2) will be fulfilled. The problems already encountered with the operator $\mathbf{\Gamma}$ (see section 3) obviously imply that this approach must to be considered with some circumspection. It is also possible that the problem may have a solution if some deeper care is taken about the boundary conditions of the VFE scheme. The assumption of a vanishing derivative imposed at the two edges of the domain is maybe not optimal for defining a Laplacian operator since this latter will have a discontinuous response for functions with non-vanishing derivatives at the edges.
In a lesser extent, there is also a risk that that the spectrum of $\mathbf{L}^*$ is not real negative, but this is the problem of the definition of $\mathbf{L}^*$ itself.
Nevertheless, this option implies a significant amount of scientific work without a clear estimation of its relevance for practical modelling. Consequently, this option is not examined further in the following of this paper, which is devoted to preliminary examinations only. However, an happy result cannot be excluded *a priori* , and Météo-France is ready to examine the behaviour of the discretisation obtained with this option if a sketch for the design of $\mathbf{L}^*$ defined through a VFE technique is provided by ECMWF.

10.3 Defining the $\mathbf{L}^*$ from $\mathbf{G}^*$, $\mathbf{S}^*$ to fulfill (C2)

This option basically consists into inverting (C2) to define the discrete Laplacian operator. Two approaches may be distinguished. The operator $\mathbf{L}^*$ could be defined by (i) just inverting the discrete constraint (C2) or (ii) by discretising a readily inverted version of the continuous (C2) constraint. These two approaches are examined here.

(i) Inverting the discrete constraint (C2)

The discrete operator $\mathbf{A}_2$ is found to be inversible, therefore, in principle the discrete constraint (C2) can be directly inverted. Following this approach, the $\mathbf{L}^*$ operator would be defined by :

$$\mathbf{L}^*_{\mathbf{G}'^*} = \left(\frac{C_v}{R}\right)\left[\mathbf{S}^*.\mathbf{G}'^* - \frac{C_p}{C_v}(\mathbf{S}^* + \mathbf{G}'^*)\right]^{-1} \tag{68}$$

or :

$$\mathbf{L}^*_{\mathbf{S}'^*} = \left(\frac{C_v}{R}\right)\left[\mathbf{S}'^*.\mathbf{G}^* - \frac{C_p}{C_v}(\mathbf{S}'^* + \mathbf{G}^*)\right]^{-1} \tag{69}$$

The main advantage of this approach is that the full constraint (C2) itself is fullfilled, and the eigenvalues of $\mathbf{L}^*.\mathbf{A}_2^*$ are all real positive [they are in fact all equal to (R/C_v)], hence the eigenmodes of the model are not likely to be intrinsically unstable.
However, there is no formal guarantee that the operator $\mathbf{L}^*$ obtained in this way will have a real negative spectrum. Indeed the $\mathbf{L}^*_{\mathbf{S}'^*}$ seems to always have a complex spectrum and is not useable. On the other hand, $\mathbf{L}^*_{\mathbf{G}'^*}$ seems to have a negative real spectrum and hence remains a candidate for further examination.
Unfortunately, it seems that this definition of $\mathbf{L}^*_{\mathbf{G}'^*}$ results in a very unaccurate operator. As an illustration, the response of $\mathbf{L}^*_{\mathbf{G}'^*}$ applied to the function $f(\eta) = \sin(6\pi\eta)$ is depicted in Fig. 24. The result obtained with the FD version of the $\mathbf{L}^*$ operator, although maybe not optimally accurate, is also depicted for reference.
The signal is clear : the Laplacian operator defined by inverting the discrete (C2) produces a very noisy result. This seems to be incompatible with a practical use in a model. It should be noted that this noise

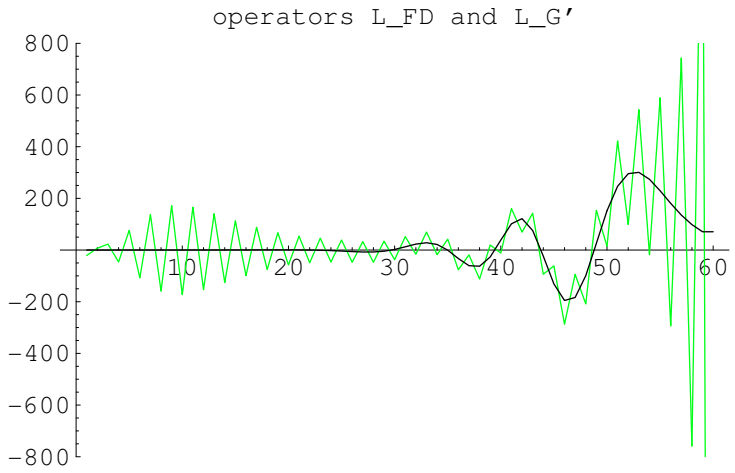

FIG. 24 – *Response of the* $\mathbf{L}^*_{\mathbf{G}'^*}$ *operator applied to the function* $f(\eta) = \sin(6\pi\eta)$*, for the ECMWF coordinate* $L = 60$*. The response of the FD version of the* $\mathbf{L}^*$ *operator (smooth curve) is superimposed for reference.*

is not present for functions which have a vanishing Laplacian at the bottom of the domain. This noise problem is maybe linked to the fact that (C2) is inversible in its discrete version but not directly in its continuous version.

We propose to abandon this option.

(ii) Inverting a readily inverted version of the continuous constraint (C2)

In the continuous context, the vertical "Laplacian" operator $\mathscr{L}$ can be defined in a unique and unambiguous way by inverting integral operators such as $\mathscr{G}$ or $\mathscr{S}$ (see Appendix 2). This property could be used to define the $\mathbf{L}^*$ operator in the discrete context by using the discrete version of this inverse operator. We then can define new Laplacian operators by :

$$\mathbf{L}^*_{\mathbf{G}'^*} = \left(\frac{C_v}{R}\right)\left[\mathbf{S}^*.\mathbf{G}'^* - \frac{C_p}{C_v}(\mathbf{S}^* + \mathbf{G}'^*)\right]^{-1}.\mathbf{C} \tag{70}$$

or :

$$\mathbf{L}^*_{\mathbf{S}'^*} = \left(\frac{C_v}{R}\right)\left[\mathbf{S}'^*.\mathbf{G}^* - \frac{C_p}{C_v}(\mathbf{S}'^* + \mathbf{G}^*)\right]^{-1}.\mathbf{C} \tag{71}$$

The response of the operators defined in such a way becomes accurate, as can be seen in Fig. 25. Moreover, the constraint (C2) is fulfiled because the eigenvalues of the $\mathbf{C}$ operator are all one or zero. Unfortunately, the spectrum of both operators $\mathbf{L}^*_{\mathbf{G}'^*}$ and $\mathbf{L}^*_{\mathbf{S}'^*}$ is found to be clearly non-real : for $\mathbf{L}^*_{\mathbf{G}'^*}$, the maximum imaginary part is about 113000, while for $\mathbf{L}^*_{\mathbf{S}'^*}$ it is about 63000, to be compared with maximum eigenvalue modules of 198000 and 146000 respectively. Such large imaginary parts are not compatible with a practical useage.

*
* *

We see that we have lost with the second approach (ii) what we have won with the first (i) : the simultaneous fulfilment of accurate response and real spectrum does not seem to be reachable using these approaches. They are consequently abandoned here as a dead-end for time being, unless new ideas are proposed.

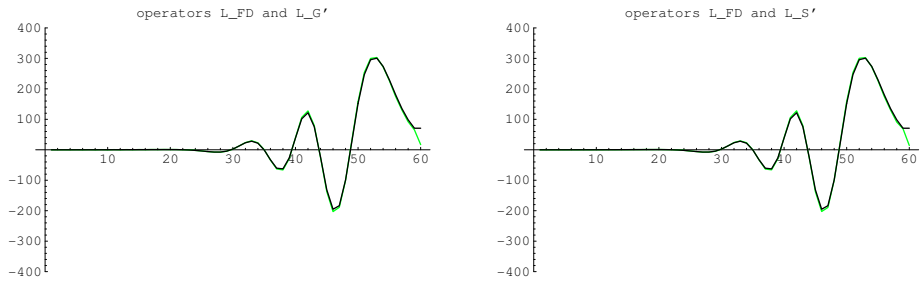

FIG. 25 – *Response of the* $\mathbf{L}^*_{\mathbf{G}'^*}$ *and* $\mathbf{L}^*_{\mathbf{S}'^*}$ *operator applied to the function* $f(\eta) = \sin(6\pi\eta)$*, for the ECMWF coordinate* $L = 60$*. The response of the FD version of the* $\mathbf{L}^*$ *operator is superimposed for reference.*

10.4 Defining the $\mathbf{L}^*$ operator in a pure FD fashion

This possibility was suggested initially because of its extreme simplicity (the amount of code changes for running the NH model would be minimal). The advantage of this option is that the behaviour of the $\mathbf{L}^*$ operator is well known and well controlled : in particular it is known that the resulting normal modes have a very simple and robust vertical structure, with clear vanishing amplitude in non-resolved areas. The disadvantage of this option is that the discrete operator $\mathbf{L}^*$ remains in its FD form, thus leading to a less accurate model than with a full VFE discretisation for the term involved with this operator.
Another disadvantage is that with this option, there is no guarantee that the eigenvalues of $\mathbf{L}^*.\mathbf{A}^*_2$ are real : in effect, when using $\mathbf{S}'^*$, the constraint (C'2) is always found to be violated, and the option is thus not relevant. When using $\mathbf{G}'^*$ however , the option seems to be applicable, but not always. From this point of view, the situation is not very clear : for regular distributions of levels, this option seems to be always relevant, and the failures are observed only for stretched coordinates. For some sets of stretched A, B values, the eigenvalues are found real and positive, while for other choices, some eigenvalues have a small imaginary part, thus preventing the use of this technique for this particular set. These failures are reminiscent of what already occured for the HPE system, in which the SI operator sometimes had a complex spectrum, but here the failure is observed for a wider set of A, B values : for instance the 60 current levels distribution of the ECMWF model leads to a violation of (C'2). It seems that a violation of the (C'2) constraint arises when the logarithmic depth $\delta\eta/\eta$ exhibits some "jumps" near the uppermost levels of the domain altogether with a high pressure resolution. However, it seems that it is always possible to modify a set of A, B values slightly in order that (C'2) becomes fulfilled, as it was in the hydrostatic case.
We don't know what to conclude about this option, since, as in the HPE case but more severely, it seems viable for some sets A, B, but not for some other ones. Maybe this option should be retained for a fast testing, facing the apparent impasse of all the other proposed options.
However, we would not recommand to retain this technique in view of long-term future NH-VFE modelling, unless the causes of the failure are better understood and possibly remedied.

10.5 Defining the $\mathbf{L}^*$ in order to fulfill (C'2), and other options

The author does not see clearly how to proceed in these two last alternative options, and leave these possibilities opened in case of any welcome suggestion.

10.6 Non-linear version of the "Laplacian" operator

The non-linear counterpart $\mathbf{L}$ of the linear operator $\mathbf{L}^*$ is present in the set of equations of the NH model, for the vertical momentum equation, where it is applied to the nonhydrostatic pressure field.
Similarly to what occured for the (C1) constraint, the (C2) constraint and more specifically the minimal sub-constraint (C'2) does not formally need to be fulfilled for the non-linear model. However a too big discrepancy between the linear operators and their non-linear version is risky, in presence of non-linear explicit residuals.
For the only option valid so far, the non-linear version of the Laplacian operator is defined naturally by simply replacing the reference-state surface-pressure by the actual surface pressure.

11 Synthesis of previous sections

At this stage, only one set of operators fulfilling all the constraints of the exercise has been found. All the other possible avenues examined has been eliminated either because they violate one of the constraints, or because they are difficult to evaluate without some further scientific work. It must be strongly outlined that the possible avenues which have been eliminated so far should not be viewed as *definitely* eliminated. In effect, further discussions may demonstrate that one or the other of these eliminated approaches is in fact a good approach, but which can be implemented in a better way. Initiating this kind of discussions is also one of the aims of this paper.
The results found in this study can be sumarized as follows :

• The current VFE scheme of the HPE IFS model is not optimally robust, and sometimes leads to an unstable linear system, when a robust model would be expected.

———

Strategies for (C1)

———

• A strategy with two coupled variables (instead of one) in the implicit problem has not been investigated here, because it was judged as too far from the current architecture of IFS/ARPEGE/Aladin codes. However, this avenue could be an interesting one for our problem.

• Options implying a redefinition of the operator $\mathbf{N}^*$ in order to fulfil (C1) have been abandoned because they lead to a 3D variable for π_s, which means deep code changes.

• For the fulfillment of (C1), the only strategies that were examined were through a redefinition of either the $\mathbf{G}^*$ or the $\mathbf{S}^*$ operator. It was found that both possibilities were relevant for the fulfillment of (C1).

• For fulfilling (C1), other strategies might be possible (as defining a VFE scheme taking into account this constraint *ab initio*), but, as fully scientific issues, they were not examined here.

———

Strategies for (C2)

———

• For (C2), all strategies based on the inversion of the operator $\mathbf{A}_2^*$ to define the operator $\mathbf{L}^*$ led to a failure : either the resulting operator $\mathbf{L}^*$ is inaccurate, or one of the two operators ($\mathbf{L}^*$, $\mathbf{L}^*.\mathbf{A}_2^*$) has a complex spectrum.

• The only possibility found so far to fulfil (C2) while having real spectra for $(\mathbf{L}^*, \mathbf{L}^*.\mathbf{A}_2^*)$, was to keep the $\mathbf{L}^*$ operator under its current FD form, thus sacrificing a bit the accuracy. It must be admitted in addition that for this strategy, the robustness has also a further degradation compared to the starting point of the HPE VFE scheme.

• As for (C1), alternative strategies consisting in a definition of a VFE scheme taking into account this constraint (C2) *ab initio* have not been examined. However, we totally miss a practical guideline for such strategies.

12 Conclusions

The aim of the present paper was to examine some of the most obvious possibilities for extending the SI-VFE discretisation from the current HPE system to the NH system in ARPEGE/IFS. It is found that most of the obvious options examined are unlikely to work in practice. The reason is that it is quite difficult to simultaneously satisfy the constraints of feasability of the algebraic elimination, accuracy, and stability of the linear system (through its eigenmodes). These constraints are much more stringent for a NH model in Euler Equation than for an HPE model, because more spatial operators are involved and especially because these operators interact in a much more intricated way.
Among the possibilities examined in this paper, only one has been found to be potentially operative, although in a not totally optimal way : it slightly sacrifices the accuracy for achieving the feasability of the SI scheme and the stability of the linear system. This possibility combines the use of VFE integral operators and a potentially less accurate FD "Laplacian" operator. This possibility also has the disadvantage to be even more subject to the "complex spectrum problem" than the current HPE version of the VFE scheme.
Moreover, it must be outlined that the present study allow to conclude only for the stability of the linear reference system used in the SI scheme, but the stability of the scheme in presence of non-linear terms is far from being automatic for the Euler Equations system (B., 2003, B. et al., 2004, B., 2004a, B. et al., 2005).
The further step in the evaluation of the potential candidate for the VFE scheme, is the study of the stability of the SI scheme in presence of non-linear terms. The technics for this study is well-controlled, but represents a significant amount of work and computations. Since the proposed candidate is not fully optimal regarding every aspects, it would be preferable to reach a consensus between ECMWF and Météo-France about the relevance of pursuing the evaluation task for this candidate, prior to undertake it effectively.
If a further evaluation of the not fully optimal proposal is not retained, possible alternatives are :

- try to produce better proposals still keeping the same strategy (algebraic elimination for the Helmholtz equation, VFE scheme designed as a NH extension of the existing HPE one). In this avenue, the most direct idea would be to define the Laplacian operator directly in a VFE fashion, independently of the constraint (C2). Of course, the minimal requirement for such an approach is that the discretised operator $\mathbf{L}^*$ has all its eigenvalues real and negative. The main risk of this approach is that the eigenvalues of $\mathbf{L}^*.\mathbf{A}_2^*$ may not be all real and positive. Since it seems difficult to predict the spectrum of an operator defined in a VFE way, we cannot estimate, at this stage, the chances of success of this approach.

- relax the current SI strategy (Helmholtz equation for a single variable) and explore SI strategies with two coupled implicit equations. The constraint (C1) then formally disappears. This approach is quite new from the point of view of both ECMWF and Météo-France practice, and also for the

circle of NWP centers, but is maybe interesting. It is difficult to estimate to which extent it can be pursued as far as a viable practical application.

- try to think the NH-VFE scheme as a totally new one, which takes into account from the beginning the fact that numerous constraints have to be fulfilled. This approach would be the most logical one, but the author does not see how to apply it from the practical point of view.

All these alternative strategies imply deeper scientific and fully original work. Therefore it is difficult to predict the effort in time and human power needed to acomplish them, and it is also difficult to evaluate the chances of success of such endeavours. It must be outlined here that, to the knowledge of the author, the task of building a SI-NH-VFE atmospheric model has not been undertaken anywhere previously. It is noticeable that the "Canadian school" which since a long time is a leader of first class in the field of SI schemes, NH models and VFE schemes has never tried to push the combination of these three elements toward a practical application.

Therefore we prefer let ECMWF examine the content of this paper, and let them make their opinion about the best strategy to follow, instead of engaging ourselves in a way which would not be consensual. Of course, any request for additional diagnosis or information from ECMWF will be kindly answered, if possible.

From the point of view of Météo-France, things are maybe easier, since a use of the combination FD-NH-SI for the global stretched application would not come up against any significant obstacle.

A possible plan for short term work could be implement first a FD-SI-NH version of the global model, for testing. Then implement the proposed solution for the extension of VFE to the NH kernel (of course only if the stability in presence of non-linear terms is confirmed by analyses). Then the scientific work for seraching better VFE operators could be pursued in parallel.

References

Bénard, P., 2003 : Stability of semi-implicit and iterative centered-implicit time discretizations for various equation systems used in NWP. *Mon. Wea. Rev.*, **131**, 2479-2491.

Bénard, P., 2004a : On the use of a wider class of linear systems for the design of constant-coefficients semi-implicit time-schemes in NWP. *Mon. Wea. Rev.*, **132**, 1319-1324.

Bénard, P., 2004b : Scientific documentation for Aladin-NH dynamical kernel. *Internal note*, available at : `http ://www.cnrm.meteo.fr/gmod/modeles/Dynamique/non_hydro/version2/designv2.ps`.

Bénard, P., R. Laprise, J. Vivoda and P. Smolíková, 2004 : Stability of the leap-frog constant-coefficients semi-implicit scheme for the fully elastic system of Euler equations. Flat terrain case. *Mon. Wea. Rev.*, **132**, 1306-1318.

Bénard, P., J. Mašek and P. Smolíková, 2005 : Stability of the leap-frog constant-coefficients semi-implicit scheme for the fully elastic system of Euler equations. Case with orography. *Accepted in Mon. Wea. Rev.*, available at : `http ://hal.ccsd.cnrs.fr/ccsd-00003241`.

Untch, A ; and M. Hortal , 2004 : A finite-element schemes for the vertical discretization of the semi-Lagrangian version of the ECMWF forecast model. *Q. J. R. Meteorol. Soc.*, **130**, 1505-1530.

Appendix 1 : Defining $\mathscr{G}'$ from (C1) in the continuous context

We will now show that in the continuous context, the set of solutions $\mathscr{G}'$ satisfying (C1) is a one dimension space. Since this space obviously contains the original $\mathscr{G}$ operator, we can say that $\mathscr{G}$ is the element of the solutions of (C1) which satisfies an additional property insuring its physical meaning, to be determined. Then this approach can be translated in the discrete context to determine a priviledged operator $\mathbf{G}'$ satisfying (C1) together with an additional property insuring its physical meaning.
In the continuous context, we first show that there is one and only one operator $\mathscr{M}$ such as

$$\mathscr{M}.\mathscr{S} = \mathscr{M} \tag{72}$$

All operators are assumed to act on the set of regular (indefinitely differentiable) functions in $[0,1]$, that is noted Ω. For convenience, we define for any r in $\mathbb{R}^+$, the function ν_r pertaining to Ω by :

$$\begin{aligned} \nu_r : \quad x &\longrightarrow x^r & (73)\\ [0,1] &\longrightarrow [0,1] & (74) \end{aligned}$$

and the function $[0]$ is the null function in Ω. We define an operator $\mathscr{M}$ by :

$$\begin{aligned} \mathscr{M} : \quad f &\longrightarrow \mathscr{M}.f = f(0)\nu_0 \\ \Omega &\longrightarrow \Omega \end{aligned} \tag{75}$$

in other words, $\forall f \in \Omega$, and $\forall x \in [0,1]$:

$$[\mathscr{M}.f](x) = f(0) \tag{76}$$

$\mathscr{M}$ satisfies (72) because $\forall f \in \Omega$, and $\forall x \in [0,1]$:

$$[\mathscr{M}.\mathscr{S}.f](x) = [\mathscr{S}.f](0) = lim_{x\to 0^+}(1/x)\int_0^x f(x')dx' = f(0) = [\mathscr{M}.f](x) \tag{77}$$

Hence we have found an operator $\mathscr{M}$ satisfying (72). We now want to demonstrate its unicity. We notice that :

$$\begin{aligned} \mathscr{S}.\nu_r &= 1/(r+1)\nu_r \quad \text{for} \quad r>0 & (78)\\ \mathscr{S}.\nu_0 &= \nu_0 & (79) \end{aligned}$$

therefore if $\mathscr{M}$ satisfies (72),

$$\begin{aligned} \mathscr{M}.\mathscr{S}.\nu_r &= [0] \quad \text{for} \quad r>0 & (80)\\ \mathscr{M}.\mathscr{S}.\nu_0 &= \nu_0 & (81) \end{aligned}$$

Now, any function f in Ω, can be written as a Taylor expansion :

$$f = \sum_i \frac{1}{i!}\frac{d^i f}{dx^i}(0)\nu_i \tag{82}$$

and therefore, if $\mathscr{M}$ satisfies (72) :

$$\mathscr{M}.f = \mathscr{M}.\mathscr{S}.f = \sum_i \frac{1}{i!}\frac{d^i f}{dx^i}(0)\mathscr{M}.\mathscr{S}.v_i = f(0)v_0 \tag{83}$$

This demonstrate the existence and unicity of $\mathscr{M}$ satisfying (72) and defined by (75). Then if we have two operators $\mathscr{G}$ and $\mathscr{G}'$ statisfying (C1), we have :

$$(\mathscr{G}' - \mathscr{G}) = (\mathscr{G}' - \mathscr{G}).\mathscr{S} \tag{84}$$

and therefore :

$$\mathscr{G}' = \mathscr{G} + \alpha\mathscr{M} \tag{85}$$

Among all the solution obtained by inverting (C1), we can then choose $\mathscr{G}'$ as the operator which is physically meaningfull, that is, the one which satisfies an additional physical constraint such as e.g. :

$$\mathscr{G}'.v_0 = \mathscr{G}.v_0 \tag{86}$$

which is referred to as the "gauge" condition in the text.

Appendix 2 : Defining $\mathscr{L}$ from (C2) in the continuous context

In this section we show that for a given function $f(\eta)$, we can define $\mathscr{L}.f$ uniquely by mean of the operator $\mathscr{A}_2$, defined by :

$$\mathscr{A}_2 = \left[\mathscr{S}.\mathscr{G} - \frac{C_p}{C_v}(\mathscr{S}+\mathscr{G})\right] \tag{87}$$

First, we notice that for a given function $f(\eta)$, the equation :

$$\mathscr{A}_2.F(\eta) = f(\eta) - C_0 \tag{88}$$

where $F(\eta)$ is an unknown function and C_0 is an unknown number, admits one and only one solution, which is given by :

$$F(\eta) = \frac{C_V}{R}\left[\eta^2 f''(\eta) + 2\eta f'(\eta)\right] \tag{89}$$

$$C_0 = \frac{C_V}{R}\left(f(1) + f'(1)\right] \tag{90}$$

As a consequence, the operator $\mathscr{A}_2$ is inversible in the space of functions $\widetilde{f}$ defined in $[0,1]$ such as $\widetilde{f}(1)+\widetilde{f}'(1)=0$, because in this space, there is one and only one function F such as $\mathscr{A}_2.F(\eta) = f(\eta)$. Considering this fact, we can define a linear operator $\mathscr{C}$ which transforms any function f defined in $[0,1]$ to the function $\widetilde{f}$ defined in $[0,1]$ by

$$[\mathscr{C}.f](\eta) = \widetilde{f}(\eta) = f(\eta) - [f(1) + f'(1)] \tag{91}$$

Then we can uniquely define the $\mathscr{L}$ operator by :

$$\mathscr{L} = \frac{R}{C_v}\mathscr{A}_2^{-1}.\mathscr{C} \tag{92}$$

In effect, for any given function $f(\eta)$:

$$\mathscr{L}.f = \mathscr{L}.\widetilde{f} = \mathscr{L}.\mathscr{A}_2.\mathscr{A}_2^{-1}.\widetilde{f} = \left(\frac{R}{C_v}\right)\mathscr{A}_2^{-1}.\widetilde{f} \equiv \left(\frac{R}{C_v}\right)\mathscr{A}_2^{-1}.\mathscr{C}.f \tag{93}$$

The first equality is due to the fact that $(f-\widetilde{f})$ is a constant function, the second one is due to the fact that $\mathscr{A}_2$ is inversible in the considered sub-space, and the third is due to (C2). This property can be used in the discrete context.